

“Spatiotemporal heterogeneity in diazotrophic communities reveals novel niche zonation in the East China Sea” by Guangming Mai et al.

We have taken all the comments of the Reviewer into account in the revision. Our point-by-point responses are provided below in blue fonts. Please note that all the line numbers mentioned in the response refer to those in the Marked-up Manuscript.

General comments:

Mai et al. investigated diazotroph abundance and activity in the East China Sea using qPCR and in situ incubations, and attempted to elucidate niche zonation with a maximum-entropy ecological model. While the data collection effort is acknowledged, the data analysis and discussion are regrettably inadequate. The modeling framework is introduced without sufficient explanation or validation, and the many results diverge from established patterns (e.g., this study suggests *Trichodesmium* favors low temperature and high nutrients). Inconsistent results with previous knowledge can be valuable, but the authors do not examine them critically and instead cite mostly only studies that support their observations. Consequently, the discussion remains largely descriptive and does not elucidate or discuss the physio-ecological mechanisms underlying diazotroph niche partitioning. Because reports of diazotrophy around the Kuroshio region and importance of Kuroshio intrusion are no longer novel, the modeling approach could have been the key contribution of this study. However, the absence of careful interpretation and the lack of clear validation leave the novelty and significance of the work unclear.

Response:

We thank the Reviewer for the very professional and constructive feedback. We have thoroughly revised the manuscript to address the issues and concerns, and accommodate them in so far as possible:

1. Enhanced model explanation and validation: Add detailed methodology and validation analyses for the maximum-entropy model (Section 2.5.3 and Table S4).

2. In-depth interpretation and discussion of inconsistent results with previous knowledge: Critically examine unexpected findings with expanded physiological and environmental interpretations (Section 4.3).

3. Balanced literature citation: Cite papers showing both consistent and conflicting results, and strengthen the mechanistic discussion of niche partitioning (Section 4.3).

4. Emphasis on the importance of modeling approaches: Clarify the ecological insights gained from the models in the context of Kuroshio dynamics (Section 4.3).

We believe these revisions substantially improve the rigor and impact of our work.

Major Comments:

1. Model justification and validation

The rationale for using the maximum-entropy model is not sufficiently explained, nor is its validity demonstrated. The authors should describe the model in more detail and clarify why it is appropriate for their dataset. Also, I suppose that such models are not necessarily valid for all datasets, and thus model significance validation should be done carefully. For example, Brun et al. (2015) evaluated model performance/validity using the AUC of the ROC curve and a student's *t*-test with randomizations to exclude invalid models. A comparable validation is needed here. Without it, the model results cannot be considered reliable.

Response:

We thank the Reviewer for this important point. We have added the description of maximum entropy model and its rationale in both the Introduction and Materials and Methods (Section 2.5.3). To validate the model, we followed the approach recommended by Brun et al. (2015), assessing the AUC of ROC curves and performing randomization Student's *t*-test. These analyses confirm the model's statistical significance and reliability, as summarized in Table S4.

2. Seemingly selective and sometimes inappropriate citations

References often appear cherry-picked to match the authors' results. For instance, in discussing phylotype-specific niche partitioning, they cite only studies whose outcomes align with their data, ignoring meta-analyses and culture experiments that already provide robust estimates of optimal temperature and nutrient ranges (details are mentioned in the specific comments). They should revise the citation thoroughly.

Response:

We thank the Reviewer for this important point. We have revised the manuscript to include a more comprehensive and balanced set of references, such as the meta-analyses (Jiang et al., 2025; Tang and

Cassar, 2019) and culture experiments (Knapp et al., 2012; Knapp, 2012), to better contextualize our findings.

3. RDA analysis

The RDA explains little of the variance of datasets (autumn: ~12 %, spring: ~34 %), yet the discussion relies on such weak relationship. RDA compresses relationships among multiple variables, but authors use them to claim direct correlations between specific taxa and single environmental parameters from RDA results. Also, collinearity among variables such as SRP, NO_x, and depth is not tested or reported, VIF threshold should be set and reported. The authors should (i) report overall R² and significance of their RDA, (ii) test the significance of each variable's significance and contribution in RDA. More simple analysis such as simple correlation and multiple-variable linear regression such as GLM may be better for understanding controlling factors on each diazotroph.

Response:

We thank the Reviewer for the insightful comment regarding the limitations of the RDA. We have removed the RDA entirely from the revised manuscript and replaced it with Pearson correlation analysis and significance test. This method allows us to directly evaluate the relationships between specific diazotrophs and individual environmental factors, providing a clear and statistically robust assessment of pairwise associations, thereby avoiding the multicollinearity issues inherent in the RDA. The updated correlation results are now presented and discussed as the main statistical support for our interpretations.

Line 201-203: “Pearson correlation analysis was adopted to explore relationship among *nifH* gene and transcript abundances (Log10 transformation), NFRs, environmental factors (z-score scaling), and distinct water masses (centered log ratio transformation).”.

Specific comments:

Introduction

L69–70: Note that Shiozaki et al. (2018) also examined diazotroph abundance using qPCR.

Response:

We thank the Reviewer for the comment. We have cited Shiozaki et al. (2018) in the revised manuscript.

Line 70-74: “Given the dominance of these diazotrophs in Kuroshio (Cheung et al., 2017, 2019; Lee Chen et al., 2014; Shiozaki et al. 2018; Wu et al., 2018) and a currently disproportionate research focus on the filamentous *Trichodesmium* populations in individual seasons (Jiang et al., 2017, 2019, 2023a, b; Yue et al., 2021), systematic investigation into the compositional dynamics of diazotrophs across the ECS is urgently needed.”.

L68–73: Because authors study phylotype-specific niches, the introduction should briefly describe the major unicellular diazotrophs rather than grouping them simply as “unicellular.”

Response:

We thank the Reviewer for the comment. We have added the description of the unicellular diazotrophs in the revised manuscript.

Line 67-70: “However, the influence of water mass-driven hydrographic processes on other globally distributed diazotrophs in the ECS, such as the unicellular cyanobacterial diazotroph (e.g., UCYN-B) and Haptophyta-associated nitroplasts (early-stage N₂-fixing organelles) (Coale et al., 2024; Cornejo-Castillo et al., 2024), have not been adequately examined.”.

L77: The term “ecotype” generally refers to distinct strains within a species.

Response:

We thank the Reviewer for the comment. We have replaced “ecotype” with “phylotype” in the revised manuscript.

Line 74-79: “Furthermore, water mass movements in the ECS are seasonally modulated by the East Asian monsoon (Yin et al., 2018), and the seasonal variability in current patterns is projected to be strengthened in climate models (Vélez-Belchí et al., 2013; Yang et al., 2024), thus necessitating a comprehensive understanding of how increasingly intensified water mass movements may restructure the distribution of distinct diazotrophic phylotypes in the ECS (Tang and Cassar, 2019).”.

L81-84. Because most readers should not be familiar with maximum entropy method, authors should explain the method more detail.

Response:

We thank the Reviewer for the comment. We have added the description of maximum entropy method in both the Introduction and Materials and Methods.

Line 83-90: “The Maximum Entropy model has proven particularly effective for characterizing species distribution in realized niches, even from sparse field observations (Irwin et al., 2012; Phillips et al., 2006). This model is capable of identifying multidimensional niche spaces along key environmental gradients (e.g., temperature and nutrients) through regularization that maximizes environmental dependency while minimizing observational bias (Irwin et al., 2012; Phillips et al., 2006). A major advantage of this method is its ability to operate without absence data or uniform sampling effort in space or time, making it suitable for oceanographic studies that rely on opportunistic sampling (Brun et al., 2015; Irwin et al., 2012).”.

Line 208-212: “The MaxEnt is a widely used species distribution model that estimates niches by combining presence-only species records with background-adjusted environmental data (Irwin et al., 2012). The quality predictive performance of MaxEnt allows it to effectively characterize species distributions even with limited data (Brun et al., 2015; Irwin et al., 2012).”.

L89-90: Brun et al. studied *Trichodesmium* and *Richelia* realized niche. It should be mentioned here and in the discussion.

Response:

We thank the Reviewer for the comment. We have mentioned the work of Brun et al. (2015) in both the Introduction and Discussion.

Line 94-97: “Despite the progress in modeling phytoplankton ecology in general, our understanding of the realized niches of diazotrophic communities remains fragmented, with only limited documentation on the modeling of realized niches of *Trichodesmium* and *Richelia* in the open ocean (Brun et al., 2015).”.

Line 538-540: “However, the realized niches here were slightly cooler in temperature ($\mu_{\text{temperature}} = 24.2^{\circ}\text{C}$, $\sigma_{\text{temperature}} = 3.2^{\circ}\text{C}$) but substantially higher and broader in NO_x ($\mu_{\text{NO}_x} = 2.5 \mu\text{M}$, $\sigma_{\text{NO}_x} = 2.54 \mu\text{M}$) relative to those of the open ocean (Brun et al., 2015).”.

Line 579-581: “Compared with the niche conditions suitable for open-ocean populations (temperature: 24.2°C ; NO_x : $1.38 \mu\text{M}$) (Brun et al., 2015), *Hets* inhabited niches of slightly higher

temperature but lower NO_x levels (Fig. 8A and C).”.

Materials and Methods

L103: “summer” should be “autumn.”

Response:

We thank the Reviewer for the comment. We have replaced “summer” with “autumn”.

Line 109-110: “We conducted a cross-season survey at 42 stations in the ECS aboard the research vessel *Xiang Yang Hong 18* during the 2023 autumn (October 13–30) and 2024 spring (April 9–24) (Fig. 1).”.

L114: Anderson and Sarmiento (1994) did not introduce P*. To my knowledge, Deutsch et al. (2007) is the first.

Response:

We thank the reviewer for the comment. Given the high collinearity between P* and soluble reactive phosphorus (SRP), we have deleted the questionable sentences in the revised manuscript.

L120: 200 µm mesh was used for RNA sample as well?

Response:

We thank the Reviewer for the comment. We have clarified this by adding “(prefiltered with 200 µm)” in the sentence.

Line 121-124: “Seawater samples (prefiltered with 200 µm pore size mesh) for RNA analysis were collected at 7 stations (Fig. 5) in the upper 50 m using acid-rinsed Nalgene polycarbonate bottles during the day (13:00–15:30 local time) or at night (21:40–3:40 local time) to mirror diel variations in nitrogenase reductase gene (*nifH*) expression (Church et al., 2005b; Moisander et al., 2014).”.

L122–123: Fig. 6 here is inappropriate, considering the order of figure.

Response:

We thank the reviewer for the comment. We have removed “(Fig. 6)” from the sentence.

Line 127-128: “Surface seawater was also obtained from 24 stations of the study area to

measure the rates of N₂ fixation, with details described below.”.

L147: Please provide the detection limit of the qPCR.

Response:

We thank the Reviewer for the comment. We have added the description of the detection limit of qPCR in the revised manuscript:

Line 161-163: “The detection limit of the qPCR reactions was 10 *nifH* gene copies per reaction, corresponding to approximately 56–250 copies per liter of seawater.”.

L148–150: Recent studies show that UCYN-C (Schvarcz et al. 2022, 2024) and γ -24774A11 (Tschitschko et al. 2024) are also likely diatom symbionts, almost organelle-like. This simplification should be described more carefully.

Response:

We thank the Reviewer for the comment. We have deleted the sentence and provided clarification on the diazotrophic phylotypes in the revised manuscript.

Line 143-149: “Recent studies have demonstrated UCYN-A2, UCYN-C and γ -24774A11 as nitroplasts in the haptophyte *Braarudosphaera bigelowii* (Coale et al., 2024; Cornejo-Castillo et al., 2024) and diatoms (Schvarcz et al., 2022, 2024; Tschitschko et al., 2024). In contrast, other UCYN-A sublineages such as UCYN-A1 have not yet been confirmed to possess the same defining characteristics in its association with haptophytes (Coale et al., 2024; Kantor et al., 2024). Therefore, for clarity and consistency with prior literature, we classified UCYN-A2, UCYN-C, and γ -24774A11 as distinct haptophyte/diatom nitroplasts, while designating UCYN-A1 as other UCYN-A sublineages.”.

L167: For transparency as suggested in (White et al. 2020), report the minimum quantifiable N₂-fixation rate for each data and the value for each replicate as supplementary material.

Response:

We thank the Reviewer for the comment. We have included the N₂ fixation rates and their respective detection limits for each replicate in Table S2.

Line 180-181: “The NFR was calculated according to Montoya et al. (1996), and the minimum

quantifiable NFR for each station ranged from 0.11 to 0.76 nmol N L⁻¹ d⁻¹ (Table S2) (Gradoville et al., 2017).”.

Table S2. N₂ fixation rates (NFRs) with detection limits in parentheses in the East China Sea during autumn and spring.

Station	Autumn NFR (nmol N L ⁻¹ d ⁻¹)		Spring NFR (nmol N L ⁻¹ d ⁻¹)	
	Replicate1	Replicate2	Replicate1	Replicate2
1	0.39 (0.7) ^a	0.58 (0.69) ^a	0.07 (0.56) ^a	0.16 (0.41) ^a
3	0.66 (0.12)	0.65 (0.13)	0.84 (0.39)	0.63 (0.4)
5	3.04 (0.76)	4.9 (0.72)	1.08 (0.45)	1.02 (0.48)
7	—	—	0.7 (0.37)	0.56 (0.34)
8	0.75 (0.19)	0.89 (0.13)	—	—
10	2.44 (0.18)	1.19 (0.18)	1.02 (0.28)	1.04 (0.29)
12	1.72 (0.35)	1.73 (0.34)	0.5 (0.5)	0.96 (0.47)
14	0.47 (0.17)	0.6 (0.17)	0.08 (0.36) ^a	0.44 (0.37)
16	1.67 (0.2)	1.41 (0.2)	0.68 (0.38)	0.97 (0.38)
18	0.56 (0.12)	1.53 (0.11)	1.31 (0.21)	1.39 (0.26)
20	7.47 (0.17)	5.08 (0.15)	0.53 (0.23)	0.29 (0.2)
22	1.46 (0.35)	1.68 (0.36)	1.75 (0.45)	1.59 (0.44)
24	0.89 (0.2)	0.78 (0.18)	1.25 (0.44)	0.48 (0.44)
26	0.99 (0.12)	0.91 (0.13)	1.1 (0.42)	0.66 (0.48)
28	0.5 (0.16)	0.45 (0.17)	0.78 (0.25)	0.4 (0.23)
30	3.2 (0.35)	2.41 (0.36)	0.41 (0.24)	1.64 (0.24)
31	0.58 (0.37)	0.2 (0.34) ^a	0.15 (0.48) ^a	0.36 (0.5) ^a
33	0.48 (0.27)	0.43 (0.26)	0.7 (0.25)	0.04 (0.2) ^a
35	0.26 (0.16)	0.24 (0.14)	0.7 (0.31)	0.71 (0.38)
36	0.41 (0.51) ^a	0.78 (0.47)	—	—
37	—	—	0.27 (0.22)	0.14 (0.24) ^a
38	0.16 (0.2) ^a	0.38 (0.17)	0.39 (0.24)	0.31 (0.24)
41	0.58 (0.37)	1.22 (0.31)	0.89 (0.14)	0.32 (0.25)
42	—	—	1.12 (0.16)	1.61 (0.17)

Note: ^a NFR below the detection limit. — data not available.

L179–183: Many readers will not be familiar with the MaxEnt model; provide a detailed description.

Past studies sometimes exclude absence data, did this study do the same?

Response:

We thank the Reviewer for the comment. We have added the description of MaxEnt and clarified the use of presence-only data in the revised manuscript.

Line 206-212: “Realized niches of diazotrophs in relation to environmental variables in the

ECS were determined in a combined framework implementing the Maximum Entropy (MaxEnt) (Phillips et al., 2006) and generalized additive model (GAM), as described by Irwin et al. (2012) and Xiao et al. (2018). The MaxEnt is a widely used species distribution model that estimates niches by combining presence-only species records with background-adjusted environmental data (Irwin et al., 2012). The quality predictive performance of MaxEnt allows it to effectively characterize species distributions even with limited data (Brun et al., 2015; Irwin et al., 2012).”

Line 216-234: “To address this, an integrated MaxEnt-GAM framework was applied in this study, which estimates species presence probability and abundance before combining them through multiplication. This framework has been used to identify the realized niches of marine phytoplankton such as diatoms, haptophytes and cyanobacteria in the western Pacific marginal seas (Xiao et al., 2018; Zhong et al., 2020).

Given the complicated effects of collinearity among environmental variables on multivariate models in the MaxEnt and GAM, we assessed the response of each diazotrophic phylotype to each individual environmental driver (i.e., the univariate model). The models are formulated as follows:

$$f(x) = P(y = 1|x) \times C(x) \quad (1)$$

$$P(y = 1|x) = P(y = 1)g_1(x)/g(x) \quad (2)$$

$$C(x) = \alpha + s(x) + \varepsilon \quad (3)$$

where $f(x)$ denotes the diazotroph abundance determined by a specific environment, x . The conditional probability of detecting diazotrophic phylotype in the environment, $P(y = 1|x)$, is evaluated using Bayes’ theorem of the MaxEnt. $P(y = 1)$ denotes the probability that diazotrophic phylotype would be found in a random sample. The probability distribution functions $g(x)$ and $g_1(x)$ are estimated from the environmental condition of all available background observations and from the conditions where the phylotype is present, respectively. $C(x)$ represents the estimated abundance of the diazotrophic phylotype as derived from GAM, using the same observational data as $g_1(x)$, but with abundance data (Log_{10} transformation) instead of presence-only data. The term $s(x)$ refers to a one-dimensional nonlinear function based on cubic regression splines, α is the grand mean, and ε denotes the error term.”.

L179: Define “breadth (σ).”, what does this mean?

Response:

We thank the Reviewer for the comment. We have added the description of “breadth (σ)” in the revised manuscript:

Line 249-255: “Following Irwin et al. (2012), we characterized the univariate response curves, $f(x)$, with two parameters: niche mean (μ) and breadth (σ), calculated as:

$$\mu = \frac{\int xf(x)dx}{\int f(x)dx} \quad (4)$$

$$\sigma^2 = \frac{\int (x-\mu)^2 f(x)dx}{\int f(x)dx} \quad (5)$$

We used the μ and σ of all environmental variables to define the realized niches of each diazotrophic phylotype. Here, μ represents the central environmental condition, while σ indicates the phylotype’s tolerance range for a given variable.”.

L180: After integration, how many observations (n) were included?

Response:

We thank the Reviewer for the comment. We have added the description of the observational data used in the MaxEnt-GAM framework in the revised manuscript:

Line 256-259: “Owing to limited data for some diazotrophic phylotypes, we integrated published data (Cheung et al., 2019; Sato et al., 2025; Shiozaki et al., 2018) with our own field observations in the ECS (this study plus unpublished surface data from October–November 2022 and April–May 2023). The total number of data points utilized in the MaxEnt-GAM framework for each diazotrophic phylotype was presented in Table S4.”.

Table S4. Summary of dataset size and univariate model performance for the MaxEnt-GAM framework.

Phylotype	N ^a	Temperature	Salinity	NO _x	SRP	DSi	N:P
<i>Trichodesmium</i>	242	0.74***	0.65***	0.67***	0.61***	0.63***	0.66***
Het-1	60	0.88***	0.72***	0.83***	0.75***	0.82***	0.82***
Het-2	134	0.77***	0.69***	0.77***	0.72***	0.77***	0.76***
UCYN-A1	67	0.77***	0.83***	0.85***	0.71***	0.82***	0.84***
UCYN-A2/A3/A4	38	0.75***	0.85***	0.88***	0.7***	0.87***	0.89***
UCYN-B	106	0.79***	0.73***	0.67***	0.65***	0.68***	0.71***
UCYN-C	30	0.88***	0.88***	0.94***	0.84***	0.81***	0.86***
γ -24774A11	153	0.82***	0.68***	0.75***	0.7***	0.74***	0.76***

Note: ^a Number of data points used for the MaxEnt-GAM framework. * $p < 0.05$, ** $p < 0.01$, *** $p < 0.001$.

L181: All parameter settings of MaxEnt should be clearly stated. Is it default setting?

Response:

We thank the Reviewer for the comment. We have added the description of the MaxEnt parameter settings in the revised manuscript:

Line 235-237: “We employed MaxEnt software (version 3.4.3) for model fitting and related statistics. To minimize model overfitting and complexity, threshold features were disabled (Irwin et al., 2012), while linear, quadratic, product and hinge features were enabled. All other parameters remained at default values.”.

L182: The GAM parameters is not explained and GAM result does not appear here after.

Response:

We thank the Reviewer for the comment. We have added the description of the GAM parameter settings. The GAM results have been incorporated into the niche mean (μ) and breadth (σ).

Line 220-234: “Given the complicated effects of collinearity among environmental variables on multivariate models in the MaxEnt and GAM, we assessed the response of each diazotrophic phylotype to each individual environmental driver (i.e., the univariate model). The models are formulated as follows:

$$f(x) = P(y = 1|x) \times C(x) \quad (1)$$

$$P(y = 1|x) = P(y = 1)g_1(x)/g(x) \quad (2)$$

$$C(x) = \alpha + s(x) + \varepsilon \quad (3)$$

where $f(x)$ denotes the diazotroph abundance determined by a specific environment, x . The

conditional probability of detecting diazotrophic phylotype in the environment, $P(y = 1|x)$, is evaluated using Bayes' theorem of the MaxEnt. $P(y = 1)$ denotes the probability that diazotrophic phylotype would be found in a random sample. The probability distribution functions $g(x)$ and $g_1(x)$ are estimated from the environmental condition of all available background observations and from the conditions where the phylotype is present, respectively. $C(x)$ represents the estimated abundance (Log_{10} transformation) of the diazotrophic phylotype as derived from GAM, using the same observational data as $g_1(x)$, but with abundance data instead of presence-only data. The term $s(x)$ refers to a one-dimensional nonlinear function based on cubic regression splines, α is the grand mean, and ε denotes the error term.”.

Line 249-255: “The GAMs with default settings were similarly applied to the same bootstrapped samples using abundance data (Log_{10} transformation).

Following Irwin et al. (2012), we characterized the univariate response curves, $f(x)$, with two parameters: niche mean (μ) and breadth (σ), calculated as:

$$\mu = \frac{\int xf(x)dx}{\int f(x)dx} \quad (4)$$

$$\sigma^2 = \frac{\int (x-\mu)^2 f(x)dx}{\int f(x)dx} \quad (5)$$

We used the μ and σ of all environmental variables to define the realized niches of each diazotrophic phylotype. Here, μ represents the central environmental condition, while σ indicates the phylotype's tolerance range for a given variable.”

L191: Z-score-scaling applied to PCA, as well?

Response:

We thank the Reviewer for the comment. We have clarified the use of Z-score scaling in PCA in the revised manuscript.

Line 260-261: “Principal component analysis (PCA) was utilized to discern the relationships between diazotrophic phylotypes and the realized niches (z-score scaling).”.

L193–194: Please clarify the VIF threshold used to avoid multicollinearity.

Response:

We thank the Reviewer for the comment. In our study, Pearson correlation analysis coupled with significance test was used to examine the relationship between diazotroph abundances and individual environmental factors. Since this approach does not require assessing the variance inflation factor (VIF) of the environmental variables, VIF analysis was not performed in our study.

Results

L214–216: Provide more specific spatiotemporal deviations from the Redfield ratio (16).

Response:

We thank the Reviewer for the comment. We have extended the description about spatiotemporal deviations from the Redfield ratio (16) in the revised manuscript.

Line 287-290: “The N:P ratio exhibited a lower range in autumn (1.3–19.5) compared to spring (0.4–37.3), but exceeded the Redfield ratio (16) in coastal waters in both seasons (autumn: 18.2 ± 1.18 at stations 1, 22 and 31; spring: 25.7 ± 6.98 at stations 1, 4, 12, 13, 14, 21 and 31), mirroring the spatial distribution pattern of NO_x (Fig. 2E and J).”.

L222: Because *nifH* was not comprehensively amplified, “*nifH* gene pool of targeted diazotrophs” is more appropriate.

Response:

We thank the Reviewer for the comment. For precision, we have revised manuscript accordingly.

Line 296-298: “*Trichodesmium* accounted for approximately 90% of the *nifH* gene pool of the targeted diazotrophs in the ECS, with both the surface and depth-integrated abundances increasing along the coast-to-offshore transects.”.

L223–225: Present quantitative numerical values.

Response:

We thank the Reviewer for the comment. We have added quantitative numerical values in the revised manuscript.

Line 298-301: “Additionally, Hets (Het-1: 11533 ± 11039 copies L^{-1} ; Het-2: 5439 ± 7317 copies

L⁻¹), UCYN-B (9107 ± 13009 copies L⁻¹) and γ -24774A11 (1961 ± 2316 copies L⁻¹) were found primarily in the southeastern ECS, with 1–2 orders of magnitude lower in abundance than *Trichodesmium*.”.

L238: Transects A and B should be mentioned in Methods and figures 1.

Response:

We thank the Reviewer for the comment. We have marked transects A and B in Figure 1 and have also referenced these transects in the Materials and Methods.

Line 128-129: “Additionally, two transects (A and B) spanning from nearshore to offshore waters were chosen to analyze vertical gradients of biological and environmental factors (Fig. 1).”.

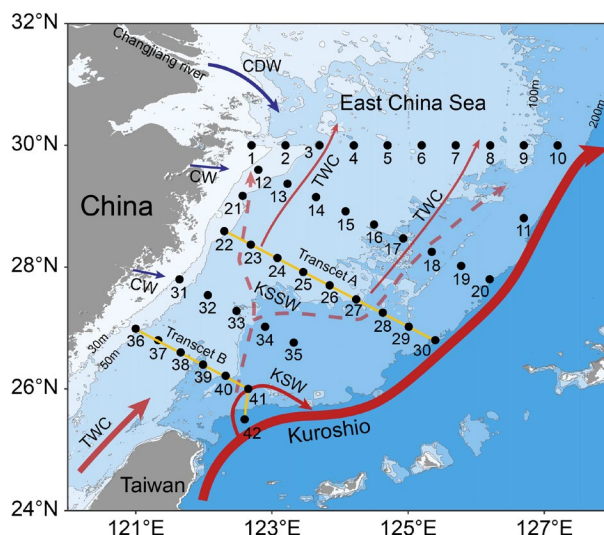


Figure 1. Sampling in the East China Sea (ECS) during the 2023 autumn and 2024 spring cruises. A total of 42 stations along 5 transects were selected for the collection of biological samples and environmental parameters. The station numbers are positioned adjacent to corresponding points. Transects A (yellow line, stations 22–30) and B (yellow line, stations 36–42) were chosen to investigate variations in biological and environmental factors along the vertical gradient extending from inshore to offshore. Major circulations are indicated, including the Changjiang diluted water (CDW), Coastal water (CW), Taiwan warm current (TWC), Kuroshio current, Kuroshio surface water (KSW) and Kuroshio subsurface water (KSSW, dashed arrows) (Yang et al., 2012, 2018). Arrow sizes denote specific discharge rates (Liu et al., 2021). Land topography and ocean bathymetry data were obtained from the General Bathymetric Chart of the Oceans (GEBCO, <https://www.gebco.net/>, last access: 24 January 2025).

L242–243: The term “broader” is vague; specify how many of how many stations, or give quantitative metrics.

Response:

We thank the Reviewer for the comment. We have added the number of stations detected for Het-1 and Het-2.

Line 318-320: “Among them, Het-2 showed a broader distribution (detected at 47 stations in autumn and 38 stations in spring) than Het-1 (12 stations per season) and peaked in the subsurface (30-m depth) (Fig. 4, S4E–L).”.

L243: UCYN-A, UCYN-C, and γ -24774A11 are now recognized as likely symbionts/organelles; grouping them as “unicellular diazotrophs” is questionable.

Response:

We thank the Reviewer for the comment. We have removed “unicellular diazotrophs” from the sentence.

Line 320-324: “The diatom symbionts/organelles (i.e., UCYN-C and γ -24774A11) were most abundant ($>10^3$ copies L^{-1}) at depths of 0–50 m (Fig. 4, S4U–Z), demonstrating moderately deeper distributions than Hets. UCYN-A2/A3/A4 was similar to *Trichodesmium* in vertical distribution but with lower abundances ($\sim 10^4$ copies L^{-1}) in spring, while UCYN-A1 and UCYN-B reached their highest abundance ($>10^4$ copies L^{-1}) at depths of 0–30 m (Fig. S4M–T).”.

L243–245: This description conflicts with Fig. 5 (4). Het-2 peaks in the subsurface, and UCYN-A2/A3/A4 show profiles similar to *Trichodesmium*.

Response:

We thank the Reviewer for the comment. We have revised the sentences accordingly.

Line 318-320: “Among them, Het-2 showed a broader distribution (detected at 47 stations in autumn and 38 stations in spring) than Het-1 (12 stations per season) and peaked in the subsurface (30-m depth) (Fig. 4, S4E–L).”.

Line 321-324: “UCYN-A2/A3/A4 was similar to *Trichodesmium* in vertical distribution but with lower abundances ($\sim 10^4$ copies L^{-1}) in spring, while UCYN-A1 and UCYN-B reached their highest abundance ($>10^4$ copies L^{-1}) at depths of 0–30 m (Fig. S4M–T).”.

L246: Sampling was not performed at 60 m. If values are interpolated, please state that and use the actual sample depth (e.g., 50 m).

Response:

We thank the Reviewer for the comment. We have replaced “60-m” with “50-m” in the revised manuscript.

Line 324-326: “Overall, diazotroph abundances decreased markedly below the 50-m layer, except for UCYN-A1 and UCYN-B which exhibited a moderate decline, possibly due to low temperature caused by KSSW intrusion (Fig. S3 and S4).”.

L251: The phrase “were the most abundant among” is unclear; perhaps “were detected as the most abundant.”?

Response:

We thank the Reviewer for the comment. We have replaced “were the most abundant” with “were detected as the most abundant” in the revised manuscript.

Line 330-333: “In autumn, the *nifH* transcripts of *Trichodesmium* were detected as the most abundant among 6 of the 7 stations sampled, ranging from 6.8×10^3 to 1.7×10^5 *nifH* transcripts L^{-1} at surface and from 5.1×10^4 to 2.4×10^6 *nifH* transcripts m^{-2} in the upper 50 m (Fig. 5A and C).”.

L269, L272: “CDW/CW-affected regions” should be defined quantitatively, e.g., by proportion of water masses.

Response:

We thank the Reviewer for the comment. We have clarified the definition of the CDW/CW-affected regions by including the proportion of water masses in the revised manuscript.

Line 352-354: “In both seasons, the rates were higher at Kuroshio-influenced stations (e.g., 20, 30 and 42), but lower in the CDW/CW-affected regions (>60% of water mass; e.g., stations 1 and 31; Fig. S2A, C, E and G).”.

L270: Figure 6 does not have station 1.

Response:

We thank the Reviewer for the comment. We have updated Figure 6 in the revised manuscript.

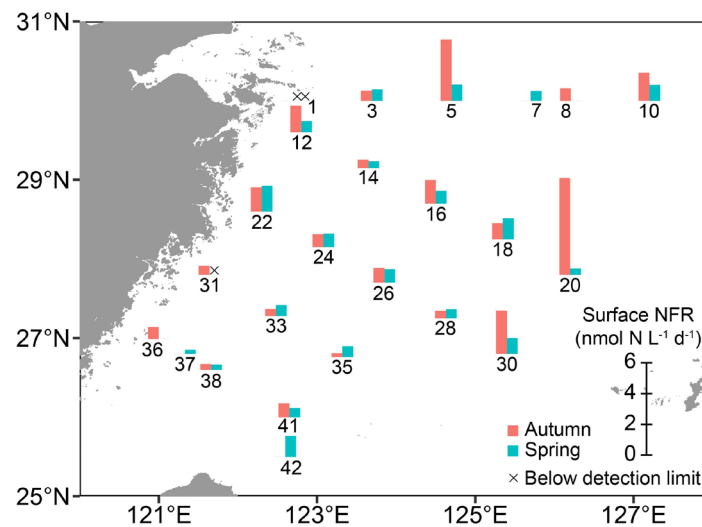


Figure 6. N_2 fixation rates in surface waters at designated stations in the ECS during autumn and spring as determined with in situ isotope tracing. The station numbers are positioned adjacent to corresponding bar charts and crossover points. Sampling excluded stations 7, 37 and 42 in autumn, and stations 8 and 36 in spring. Land topography was obtained from the General Bathymetric Chart of the Oceans (GEBCO, <https://www.gebco.net/>, last access: 24 January 2025).

L271: “About 60%” is more appropriate.

Response:

We thank the Reviewer for the comment. After re-evaluating the NFRs, which yielded a value of 54.8% (0.74/1.35), we feel that describing this proportion as “half” is now appropriate.

Line 349-352: “In autumn, the NFRs ranged from undetectable to $6.28 \text{ nmol N L}^{-1} \text{ d}^{-1}$ ($1.35 \pm 1.45 \text{ nmol N L}^{-1} \text{ d}^{-1}$ on average). In spring, the NFRs ranged from undetectable to $1.67 \text{ nmol N L}^{-1} \text{ d}^{-1}$ ($0.74 \pm 0.42 \text{ nmol N L}^{-1} \text{ d}^{-1}$ on average) and were about half of the autumn rates on average.”.

L276–277: To support this, I recommend to perform multivariable regression for each phylotype and report the coefficients of determination, so that importance of each variable can be quantified.

Response:

We thank the Reviewer for the suggestion. In our study, we used Pearson correlation analysis to examine the relationships between diazotroph abundances and environmental variables, including centered log ratio-transformed water masses. As a parametric method, Pearson correlation analysis is effective for identifying linear associations, which aligned with our goal of directly linking diazotroph distributions with distinct water masses. The resulting correlation coefficients are analogous to R^2 values

in regression, effectively quantifying the strength and direction of each variable’s link with phylotypes.

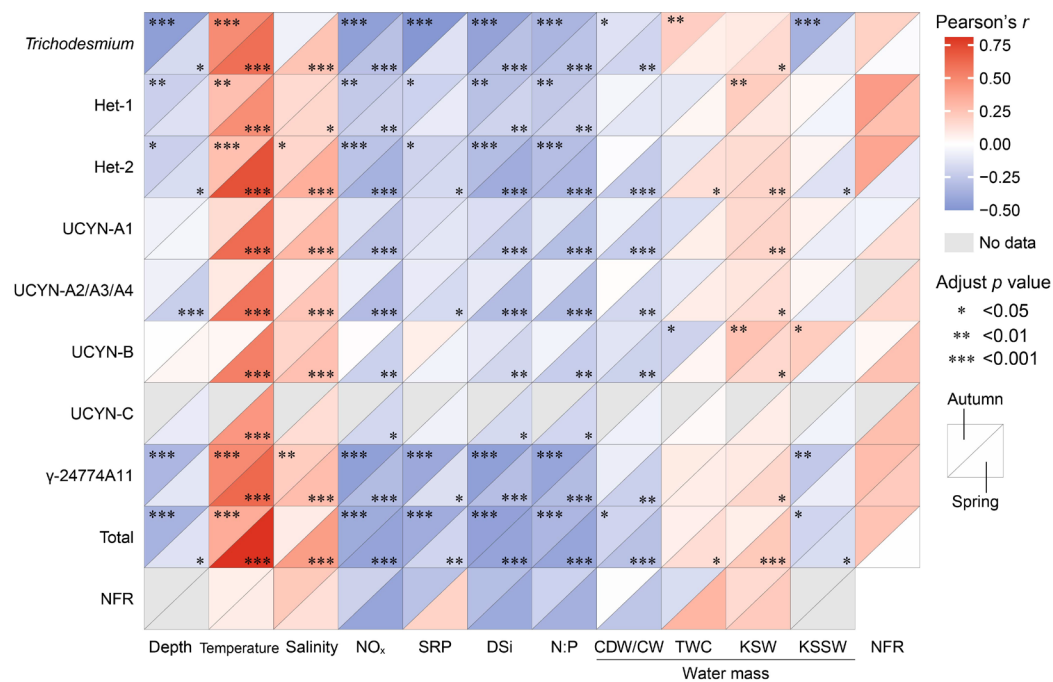


Figure 7. Pearson correlation between diazotroph abundances, N_2 fixation rates and environmental variables, including water masses, in the ECS. Total, total *nifH* gene abundances of eight diazotrophs that detected.; CDW, Changjiang diluted water; CW, Coastal water; TWC, Taiwan warm current; KSW, Kuroshio surface water; KSSW, Kuroshio subsurface water.

L281: Figure S6 should be moved into the main text; otherwise readers cannot follow the discussion of μ and σ . Also, please evaluate model validity as mentioned in major comments.

Response:

We thank the Reviewer for the suggestion. We have merged the former Figures 8 and S6 into a new Figure 8 and have added the description of model validity in the revised manuscript.

Line 370-379: “Prior to the MaxEnt-GAM framework, model performance for the realized niches of each diazotrophic phylotype in relation to each individual environmental factor was assessed using AUC scores from MaxEnt. The AUC values ranged from 0.61 to 0.94 across diazotrophic phylotypes and environmental variables, with an average of 0.77 (Table S4), suggesting better predictive accuracy of the univariate models than the random predictions. Notably, UCYN-C achieved the highest model performance with an average AUC of 0.87 across all the variables, likely due to the relatively small dataset ($N = 30$; Table S4). In contrast, *Trichodesmium* yielded the lowest average AUC (0.66), which may be attributed to its larger sample

size (N = 242).

We characterized the realized niche mean (μ) and breadth (σ) of diazotrophs in the ECS with combined hydrographic, environmental and biological data, identifying three distinct clusters among the diazotrophs (Fig. 8 and S6).”.

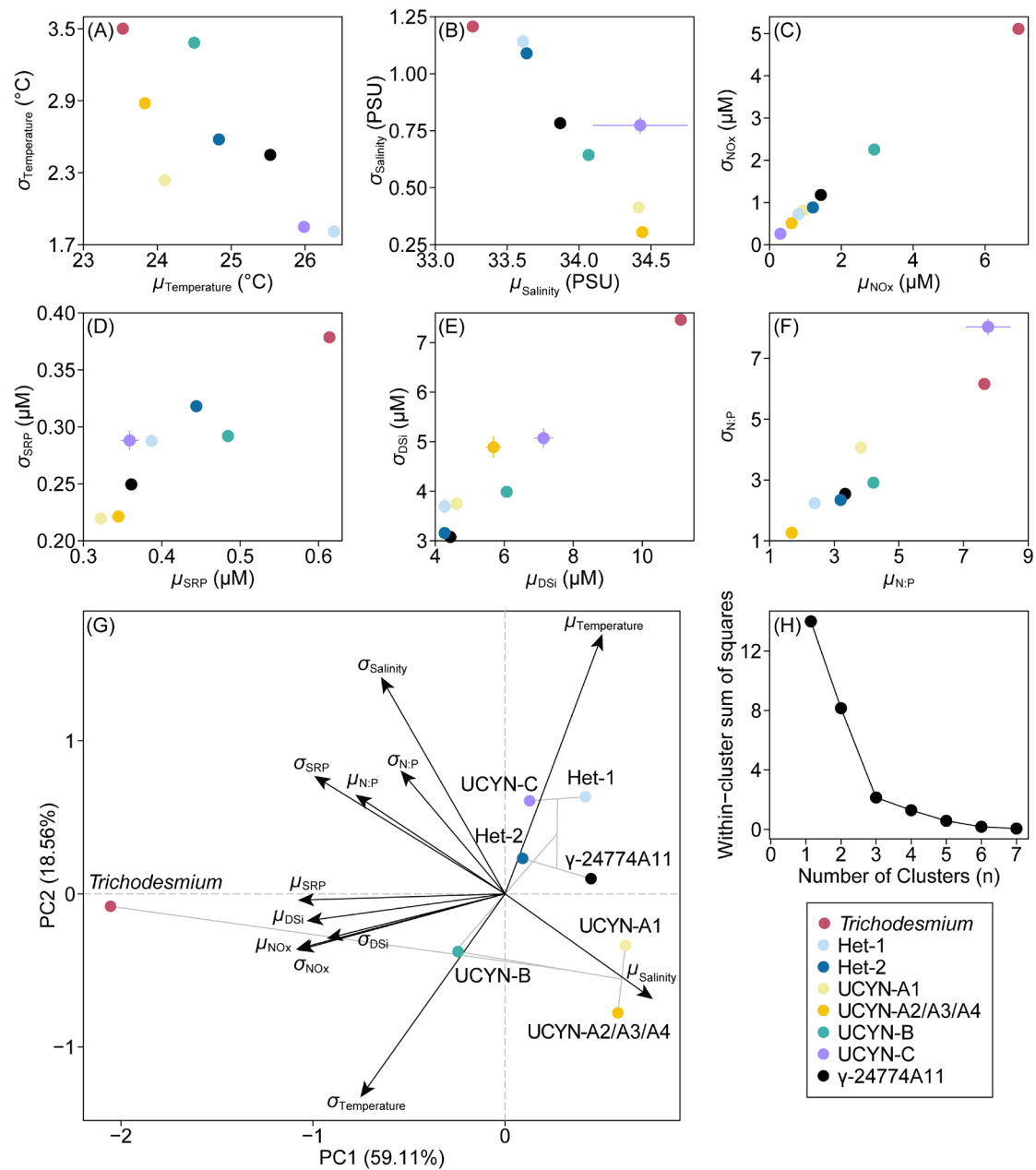


Figure 8. Scatter plots (A–F) and principal component analysis (G) depicting niche mean (μ) and breadth (σ) of each diazotrophic phylotype relative to environmental variables in the East China Sea. Lines (A–F) across the data points indicate 95% confidence intervals for each variable derived from 1000 bootstrap resampling. Clustering (G) among the diazotrophs is shown in grey lines. Elbow plot (H) for determining the optimal clusters based on within-cluster sum of squares.

Table S4. Summary of dataset size and univariate model performance for the MaxEnt-GAM framework.

Phylotype	N ^a	Temperature	Salinity	NO _x	SRP	DSi	N:P
<i>Trichodesmium</i>	242	0.74***	0.65***	0.67***	0.61***	0.63***	0.66***
Het-1	60	0.88***	0.72***	0.83***	0.75***	0.82***	0.82***
Het-2	134	0.77***	0.69***	0.77***	0.72***	0.77***	0.76***
UCYN-A1	67	0.77***	0.83***	0.85***	0.71***	0.82***	0.84***
UCYN-A2/A3/A4	38	0.75***	0.85***	0.88***	0.70***	0.87***	0.89***
UCYN-B	106	0.79***	0.73***	0.67***	0.65***	0.68***	0.71***
UCYN-C	30	0.88***	0.88***	0.94***	0.84***	0.81***	0.86***
γ -24774A11	153	0.82***	0.68***	0.75***	0.7***	0.74***	0.76***

Note: ^a Number of data points used for the MaxEnt-GAM framework. * $p < 0.05$, ** $p < 0.01$, *** $p < 0.001$.

L281: From Fig. S7, $n = 3$ seems most appropriate; consider adding a hierarchical cluster tree to illustrate the threshold objectively.

Response:

We thank the Reviewer for the comment. We have set $n = 3$ and incorporated a hierarchical cluster tree in the supplementary materials (now Figure S6), which provides an objective basis for this choice. We also have replaced “five” with “three” in the revised manuscript.

Line 377-379: “We characterized the realized niche mean (μ) and breadth (σ) of diazotrophs in the ECS with combined hydrographic, environmental and biological data, identifying three distinct clusters among the diazotrophs (Fig. 8 and S6).”.

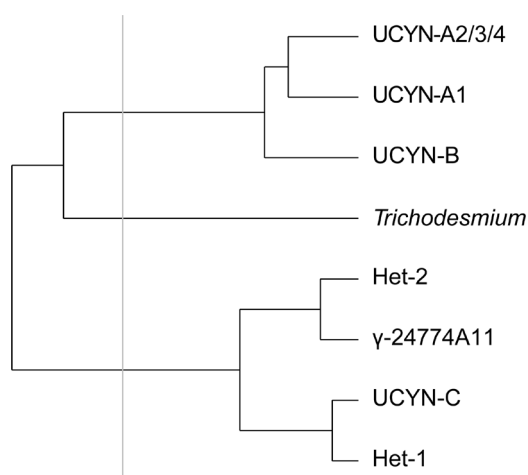


Figure S6. Hierarchical clustering of diazotrophs based on the first two PCA components, with optimal cluster number indicated by a gray line derived from elbow plot (Figure 8H).

L290: “Relatively high” should be described with quantitative data.

Response:

We thank the Reviewer for the comment. We have revised the sentence and incorporated quantitative data to clarify the result accordingly.

Line 384-387: “The diatom-diazotroph symbioses (i.e., Hets, UCYN-C and γ -24774A11) were associated with high-temperature (25.7°C on average), low-NO_x (0.98 μ M on average) and moderate-SRP conditions (0.39 μ M on average), demonstrating substantial ecological overlap among them.”.

Discussion

L295–297: Current ecological model (Fig. S6) shows *Trichodesmium* preferring low temperature, low salinity, and high nitrate waters. This contradicts both claim here and previous studies.

Response:

We thank the Reviewer for the comment. The pattern in Fig. 8 (previously Fig. S6) reflects a new and careful interpretation of our model result, which stresses statistical correlation between *Trichodesmium* distribution and environmental variables in the study region. The seemingly controversy “preference for lower temperature (Fig. 8A) and higher NO_x (Fig. 8C)” is only used to describe *Trichodesmium*’s presence in the CDW/CW-influenced waters (Fig. 2A, 3A and S2A). But more importantly, the model demonstrates that *Trichodesmium* exhibits a broad range of both temperature and NO_x tolerance (Fig. 8A and C), suggesting its ability to survive in both cool, NO_x-rich and warm, NO_x-poor waters. On the warm, NO_x-depleted outer ECS shelf, the capability of nitrogen fixation is advantageous to *Trichodesmium* distribution, which outcompete non-diazotrophs under severe nitrogen limitation. Thus, the model unfolds the whole picture of *Trichodesmium* habitats. Our observation is overall consistent with previous knowledge on *Trichodesmium* physiology, in the conclusion that nitrogen limitation is the key factor enabling its preference in the oligotrophic outer ECS shelf. We have also clarified this competitive advantage of *Trichodesmium* under the warm, NO_x-depleted waters in the revised manuscript.

Line 405-408: “Notably, while our modeling result indicated *Trichodesmium* can survive in relatively cool (23.5°C), NO_x-rich environments (6.93 μ M; Fig. 8), it was detected the most abundant in the warm, NO_x-depleted outer ECS shelf (Fig. 3), a pattern that is consistent with the

basal physiology of *Trichodesmium* (Brun et al., 2015; Jiang et al., 2025; Tang and Cassar, 2019).”.

L298: growth was not measured in this study.

Response:

We thank the Reviewer for the comment. We have removed "growth" from the sentence in the revised manuscript.

Line 394-396: “In contrast, their abundances were considerably lower in the cold, NO_x-rich coastal waters influenced by the CDW/CW (Fig. S2A and E), showing positive correlation with temperatures but negative correlation with nutrient concentrations and N:P ratios (Fig. 7).”.

L300–301: Relationships inferred from RDA are weak and not checked stastically.

Response:

We thank the Reviewer for the comment. We have replaced the RDA with Pearson correlation analysis, supplemented with statistical significance test.

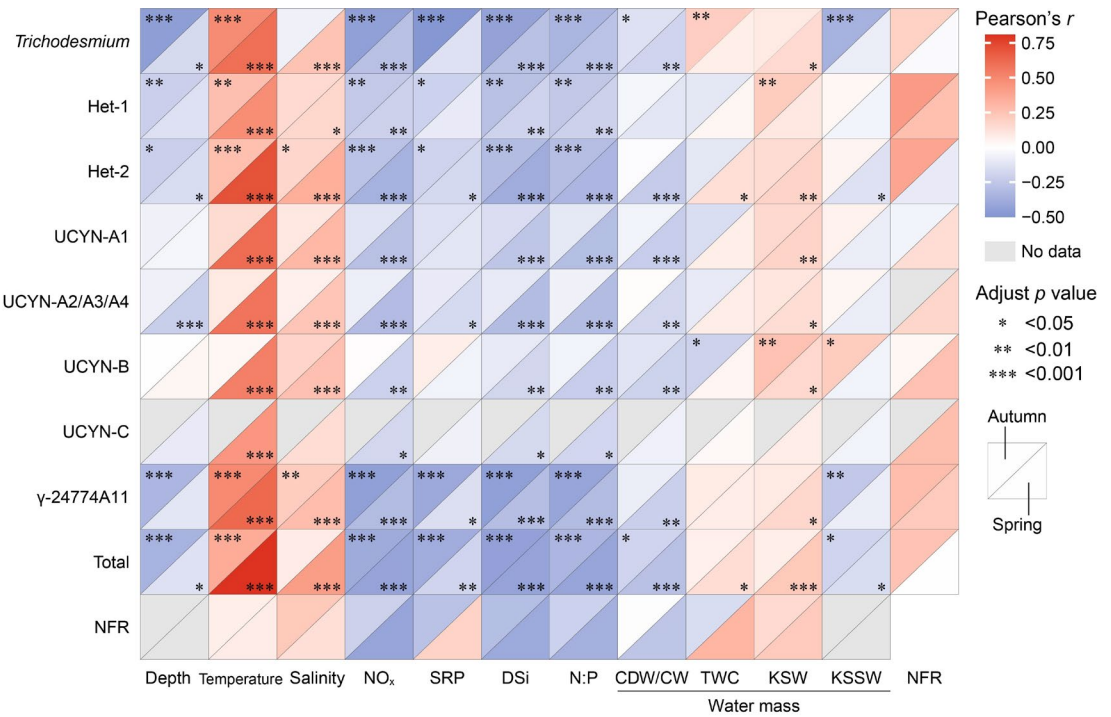


Figure 7. Pearson correlation between diazotroph abundances, N₂ fixation rates and environmental variables, including water masses, in the ECS. Total, total *nifH* gene abundances of eight diazotrophs that detected.; CDW, Changjiang diluted water; CW, Coastal water; TWC, Taiwan warm current; KSW, Kuroshio surface water; KSSW, Kuroshio subsurface water.

L303: “Below detection limit” does not mean complete absence.

Response:

We thank the Reviewer for the comment. We have replaced “but complete absence” with “while these phylotypes were not detected” in the revised manuscript.

Line 409-411: “Additionally, non-filamentous diazotrophs (UCYN-A, UCYN-B, UCYN-C and γ -24774A11) were abundant ($>5 \times 10^4$ *nifH* gene copies L^{-1}) in Kuroshio-influenced waters, but not detectable in the CDW/CW-dominated regions (Fig. 3 and S2).”.

L307–309: Conclusions based solely on weak RDA correlations are too qualitative.

Response:

We thank the Reviewer for the comment. We have replaced the RDA with Pearson correlation analysis, supplemented with statistical significance test.

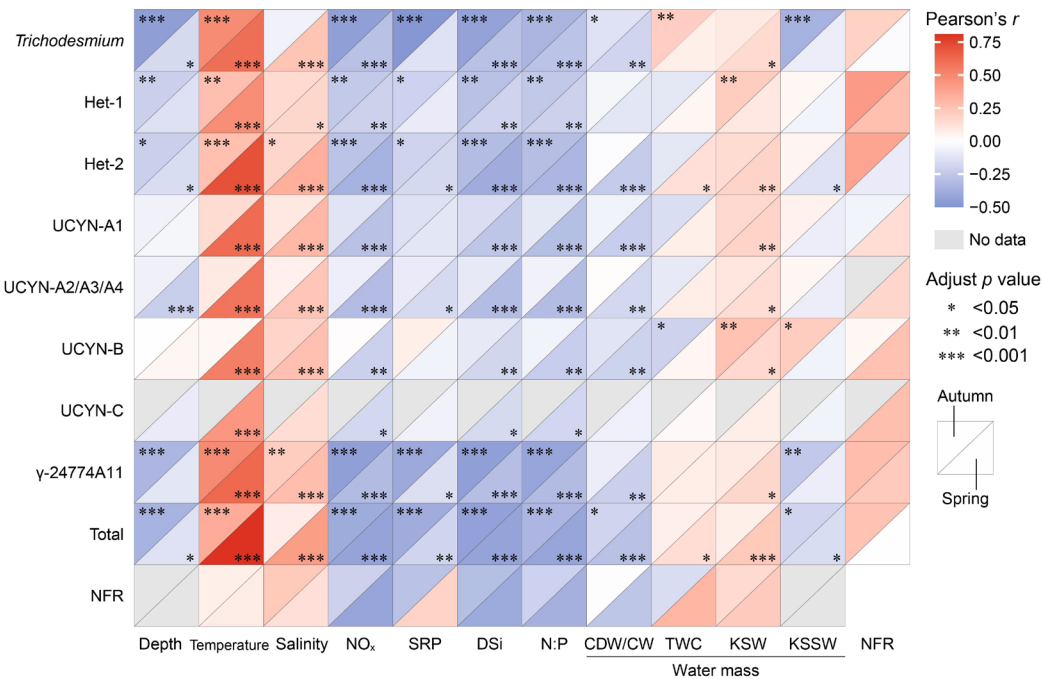


Figure 7. Pearson correlation between diazotroph abundances, N_2 fixation rates and environmental variables, including water masses, in the ECS. Total, total *nifH* gene abundances of eight diazotrophs that detected.; CDW, Changjiang diluted water; CW, Coastal water; TWC, Taiwan warm current; KSW, Kuroshio surface water; KSSW, Kuroshio subsurface water.

L309–311: To demonstrate major N₂ fixers, statistically test relationships between gene (or transcript) abundance and N₂-fixation rate. High *nifH* abundance alone is insufficient.

Response:

We thank the Reviewer for the comment. We have performed Pearson correlation analysis to assess the relationship between diazotroph abundances and N₂ fixation rates in the revised manuscript.

Line 416-421: “Overall, filamentous diazotrophs were the primary N₂ fixers in the ECS (Jiang et al., 2023a, b), as illustrated by the prevalence of their *nifH* gene (~84% of all the *nifH* copies detected; Fig. 3) that was positively correlated with NFRs (Fig. 7) across most of the surveyed areas. On the other hand, UCYN-A1, UCYN-B and γ -24774A11 were only occasionally found in the Kuroshio-influenced regions (Fig. 3 and S2), and the correlation of their *nifH* gene abundances with NFRs (Fig. 7) suggests their potential contribution to regional N₂ fixation (Lee Chen et al., 2014; Wu et al., 2018).”.

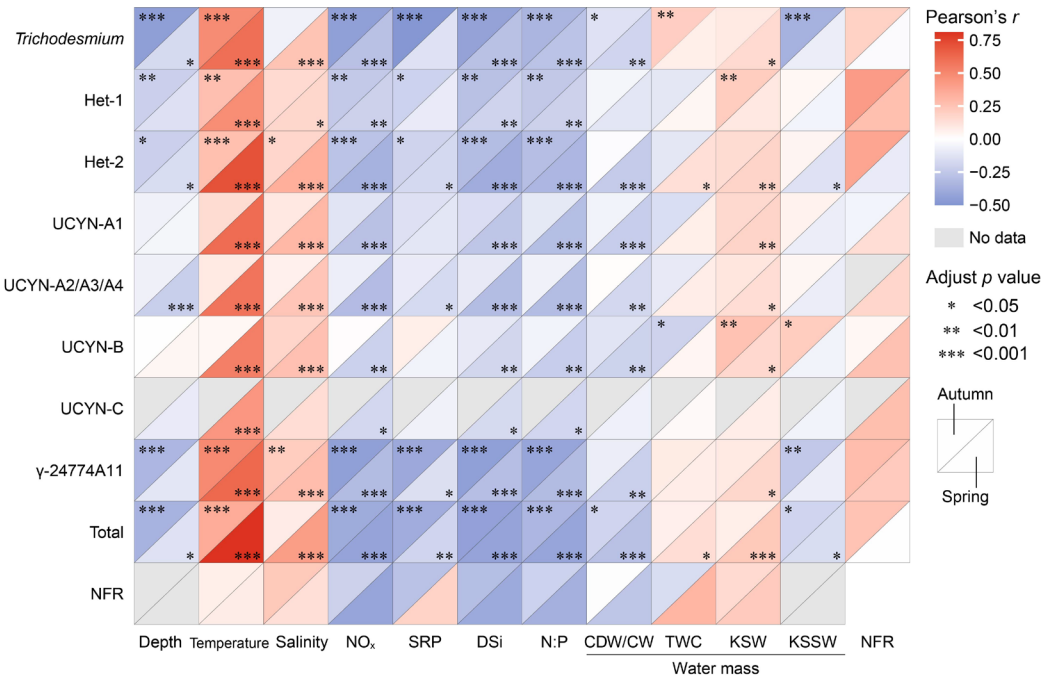


Figure 7. Pearson correlation between diazotroph abundances, N₂ fixation rates and environmental variables, including water masses, in the ECS. Total, total *nifH* gene abundances of eight diazotrophs that detected.; CDW, Changjiang diluted water; CW, Coastal water; TWC, Taiwan warm current; KSW, Kuroshio surface water; KSSW, Kuroshio subsurface water.

L314–315: Many studies detected *Trichodesmium* colonies in the ECS (e. g. Marumo and Asaoka 1974, Jiang et al. 2023). *Richelia* colonies are also expected to be removed by this mesh filtering. Was microscopy performed in this study? They should provide more solid evidence of not-underestimating, otherwise it is not convincing.

Response:

We completely agree with the reviewer that prefiltration using a 200 μm pore-size nylon mesh may potentially remove large colonies of *Trichodesmium* and *Richelia*. As microscopy was not performed, we have revised the Discussion section to explicitly state that the abundance for these colonial diazotrophs may be underestimated.

Line 422-423: “It should be noted that the abundance of colonial diazotrophs like *Trichodesmium* and *Hets* may be potentially underestimated due to the use of <200- μm size fraction in our study (e.g., Jiang et al., 2023a).”.

L319: Jiang et al. (2018, 2019) reported highest densities at the surface and 10–50 m, consistent with your results. Carpenter et al. (2004) also found maxima at ~20 m. Discussion here seems incorrect.

Response:

We thank the Reviewer for the comment. We have revised the sentence accordingly.

Line 425-428: “Specifically, *Trichodesmium* showed maximum abundance in the upper 30 m (Fig. S4A–D), consistent with earlier reports of surface or subsurface maxima (10–30 m) in the ECS (Jiang et al., 2018, 2019) and other regions (Carpenter et al., 2004; Lee Chen et al., 2003; Lu et al, 2019).”.

L323: If eddy is important, provide and check the SSH and its anomaly information during study period.

Response:

We thank the Reviewer for the comment. We have included the sea surface height anomaly and geostrophic current vectors during the study period in Figure S7 in the revised manuscript.

Line 430-432: “Additionally, the absence of anticyclonic eddies during our surveys is likely to eliminate the downward entrainment of *Trichodesmium* in deeper water column (e.g., 50–60 m) (Fig. S7) (Jiang et al., 2018).”.

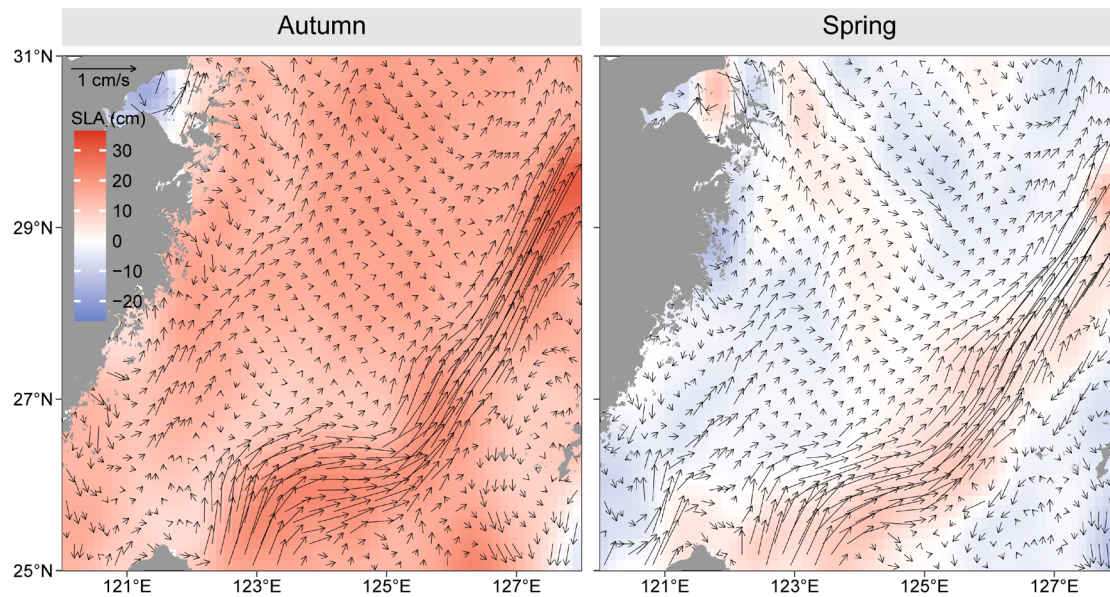


Figure S7. Average sea level anomaly (SLA, cm) and geostrophic current vectors (arrows) in the East China Sea during autumn and spring cruises. The SLA and current data were obtained from Copernicus Marine and Environment Monitoring Service website (<http://marine.copernicus.eu/>), and land topography was obtained from the General Bathymetric Chart of the Oceans (GEBCO, <https://www.gebco.net/>, last access: 24 January 2025).

L324: Only UCYN-C and γ -24774A11 peak at 50 m; others peak above 30 m. Thus filamentous and unicellular diazotrophs are not “in contrast.”

Response:

We thank the Reviewer for the comment. We have revised the sentences accordingly.

Line 425-447: “Specifically, *Trichodesmium* showed maximum abundance in the upper 30 m (Fig. S4A–D), consistent with earlier reports of surface or subsurface maxima (10–30 m) in the ECS (Jiang et al., 2018, 2019) and other regions (Carpenter et al., 2004; Lee Chen et al., 2003; Lu et al, 2019). This depth distribution may be attributed to favorable nutrient conditions (e.g., SRP and iron) and light intensity (Turk-Kubo et al., 2018; Wen et al., 2022), which support *Trichodesmium* growth on the site of the ongoing surveys (Fig. 2D and I). Additionally, the absence of anticyclonic eddies during our surveys is likely to eliminate the downward entrainment of *Trichodesmium* in deeper water column (e.g., 50–60 m) (Fig. S7) (Jiang et al., 2018). The filamentous diazotrophs Het-1 and Het-2 showed distinct maximum depths (surface versus 30 m; Fig. 4), contrasting with previously documented subsurface maxima (10–40 m) for both phylotypes in the ECS (Jiang et al., 2019), the tropical North Atlantic (Foster et al., 2007; Goebel et al., 2010) and the western tropical South Pacific (Stenegren et al., 2018). This may be due to different habitat

preferences between the Het hosts, as the Het-1 host was found mainly under NO_x-depleted conditions but not in the deeper, NO_x-repleted water column (Tuo et al., 2014). Alternatively, the differences in thermal sensitivity between Het-1 and Het-2 may explain their vertical distribution, as Het-1 lives within a relatively narrower temperature range (20.4–27.5°C) than Het-2 (17.6–27.6°C; Fig. S3). In contrast, the other two diatom-diazotroph symbioses (UCYN-C and γ -24774A11) showed both surface and subsurface maxima (~50 m; Fig. 4). The deep distributions may result from the low light tolerance of their diatom hosts, as both symbionts lack photosynthetic pigments and rely entirely on carbon fixed by their hosts (Schvarcz et al., 2022, 2024; Tschitschko et al., 2024). Similar subsurface distributions have been observed in UCYN-C at Station ALOHA (Schvarcz et al., 2022) and γ -24774A11 in the northern South China Sea (SCS; Chen et al., 2019; Lu et al., 2019; Shao and Luo, 2022).

Similar to the filamentous diazotrophs, UCYN-A and UCYN-B were mostly confined to the upper 30 m, matching observations from the northern SCS (Lu et al., 2019) and global oceans (Tang and Cassar, 2019).”.

L329: Lu et al. 2018 does not seem to provide the information of light adaptation of unicellular cyanobacterial diazotrophs?

Response:

We thank the Reviewer for the comment. We have removed the citation of Lu et al. (2018) and revised the sentence accordingly.

Line 448-450: “However, UCYN-A1 and UCYN-B were moderately abundant (~10³ copies L⁻¹) in deep layers (Fig. S4M, N, Q–T), potentially due to their low light saturation coefficients (Garcia et al., 2013; Gradoville et al., 2021; Shen et al., 2024).”.

L332: ~22°C for optimal temp. of UCYN-B is not common understanding. Also, Webb et al 2009 report 26–30°C for its optimal temperature. Other studies also reported ~25–30 °C (Tang and Cassar 2019; Mauda 2024).

Response:

We thank the Reviewer for the comment. We have revised the sentences and clarified UCYN-B’s persistence in cold environments in the revised manuscript.

Line 454-461: “However, such low temperatures may inhibit UCYN-B, which has an optimal growth temperature around 25–30°C (Fu et al., 2014; Jiang et al., 2025; Tang and Cassar, 2019; Webb et al., 2009). Nevertheless, studies have indicated that UCYN-B can persist in cold environments, albeit at low abundances (Jiang et al., 2025; Tang and Cassar, 2019). Low-temperature tolerance of UCYN-B has also been demonstrated in the laboratory (Deng et al. 2022), however, the lowest threshold temperature used for the bottle incubation (25°C) is substantially higher than the in situ temperatures (~10–30°C) in the field (Tang and Cassar, 2019). Therefore, the distribution of UCYN-B under such low-temperature conditions warrants further investigation.”.

L334–338: Tschitschko et al. 2024 in Nature strongly (almost conclusively) indicate that γ -24774A11 is a diatom symbiont. Include this information.

Response:

We thank the Reviewer for the comment. We have incorporated this information into the sentence accordingly.

Line 439-441: “In contrast, the other two diatom-diazotroph symbioses (UCYN-C and γ -24774A11) showed both surface and subsurface maxima (~50 m; Fig. 4).”.

L346: Koenig et al. (2009) only speculated about an r-strategy for *Trichodesmium*; they did not conclude it. Citing this paper as proof in current manner is inappropriate.

Response:

We thank the Reviewer for the comment. We have removed the citation of Koenig et al. (2009) and revised the sentence accordingly.

Line 470-474: “It has been suggested that iron deficiency limits *Trichodesmium* growth (Berman-Frank et al., 2001). Given that SRP (0.2–0.4 μ M) did not appear to be a limiting factor (Fig. 2D), the dominance of *Trichodesmium* in the ECS is likely due to the high level of dissolved iron (0.76–30 nM) transported via the Kuroshio and TWC (Shiozaki et al., 2015; Su et al., 2015) or delivered via aerial dust deposition (Guo et al., 2014).”.

L351–353: This statement seems contradict the Maxent based discussion.

Response:

We thank the Reviewer for the comment. The MaxEnt-GAM framework predicts the potential distribution based on the species' occurrence, which spans a wide range of temperatures and NO_x. However, the discussion here focuses on its ecological performance, where it becomes dominant. Although it can exist in cool, NO_x-rich waters (as shown by the MaxEnt-GAM; Fig. S4A), its abundance is significantly higher in the warm, NO_x-poor waters (i.e., preferred and dominant habitat). Thus, there is no contradiction between our statement and the MaxEnt-GAM-based discussion.

L360: Please quantitatively compare your data values with those of Jiang et al. 2023 with actual value.

Response:

We thank the Reviewer for the comment. We have included the quantitative comparison of our data with Jiang et al. (2023) in the revised manuscript.

Line 486-488: “The averaged autumn NFR (1.35 nmol N L⁻¹ d⁻¹) was close to what has been reported during summer in the ECS (1.54 nmol N L⁻¹ d⁻¹) (Jiang et al., 2023a), despite the differences in NFR measurement between the two studies (i.e., dissolution versus bubble methods).”.

L364–367: Only one phylotype of non-cyanobacterial diazotroph (NCD) was quantified. Many other NCDs likely exist; please acknowledge this limitation.

Response:

We thank the Reviewer for the comment. We have incorporated the discussion of this limitation in the revised manuscript.

Line 491-495: “On the other hand, the low temperature (14–20°C) in spring could otherwise promote the prevalence of non-cyanobacterial diazotrophs (NCDs) and their contribution to N₂ fixation, particularly in CDW/CW-affected waters (Jiang et al., 2023b), but this pattern was not comprehensively analyzed in this study since only one phylotype of NCD (γ-24774A11) was quantified with qPCR (Fig. 3 and 6).”.

L367–368: A simple correlation analysis between N₂-fixation rate and *nifH* transcript abundance is needed to support this argument.

Response:

We thank the Reviewer for the comment. We have performed Pearson correlation analysis between N₂ fixation rate and *nifH* transcript abundance and have included the results in Table S5 in the revised manuscript.

Line 495-497: “Notably, the seasonal dynamics of NFRs showed negative, but not significant, correlation with transcriptional abundances of diazotrophs (Fig. 5 and 6; Table S5), suggesting that the expression of *nifH* gene in diazotrophs may not be synchronized with actual nitrogenase activity (Turk-Kubo et al., 2012).”.

Table S5. Pearson correlation coefficients between surface N₂ fixation rates (NFRs) and diazotroph transcripts in the East China Sea.

Parameter	<i>Trichodesmium</i>	Het-1	Het-2	UCYN-A1	UCYN-A2/A3/A4	UCYN-B	γ -24774A11	Total
NFR ^a	-0.54	-0.05	-0.40	-0.26	-0.26	-0.29	-0.88	-0.66

Note: ^a NFRs and diazotroph transcript abundances from autumn and spring were pooled for Pearson correlation analysis due to scarce data in spring. Total, total *nifH* transcripts of seven diazotrophs that detected.

L370: Recent studies report cell-specific rates for UCYN-C (Schvarcz et al. 2022) and γ -24774A11 (Tschitschko et al. 2024). Also, please provide standard deviations.

Response:

We thank the Reviewer for the comment. We have incorporated the cell-specific NFRs of UCYN-C and γ -24774A11 into the calculation of bulk rates and added standard deviations of estimated NFRs in Table S6.

Line 498-499: “To assess the contribution of key diazotrophs to the N budget, we extrapolated water-column NFRs using published, cell-specific rates for the targeted diazotrophs (Table S6).”.

Table S6. The estimated N₂ fixation rate (NFR) in the East China Sea during autumn and spring derived from polyploidy factor, cell-specific NFR and the targeted diazotroph abundances. The NFRs are shown as mean ± standard deviation.

Phylotype	Polyploidy factor	Cell-specific NFR (fmol N cell ⁻¹ d ⁻¹)	Autumn NFR		Spring NFR	
			Surface	Depth integrated	Surface	Depth integrated
			(nmol N L ⁻¹ d ⁻¹)	(μmol N m ⁻² d ⁻¹)	(nmol N L ⁻¹ d ⁻¹)	(μmol N m ⁻² d ⁻¹)
<i>Trichodesmium</i>	12	53	0.73 ± 0.73	15.49 ± 12.15	0.11 ± 0.43	2.58 ± 8.67
Het-1	2.6	216	0.30 ± 0.84	7.10 ± 17.36	0.09 ± 0.35	3.97 ± 19.10
Het-2	2.6	216	0.18 ± 0.48	10.42 ± 22.46	0.09 ± 0.22	4.45 ± 11.74
UCYN-A1	14	2.7	0.00009	0.007	0.002 ± 0.01	0.11 ± 0.38
UCYN-A2	14	55	—	0.01 ± 0.04	0.01 ± 0.01	0.14 ± 0.38
UCYN-B	3.6	12.4	0.02 ± 0.04	0.86 ± 2.16	0.01 ± 0.02	0.28 ± 0.86
UCYN-C	1	92.4	—	—	0.04 ± 0.16	1.79 ± 8.37
γ-24774A11	1	162.5	0.23 ± 0.39	10.26 ± 16.18	0.26 ± 0.80	16.19 ± 63.48

Note: Average polyploidy factors for each diazotrophic phylotype were obtained from Shao et al. (2023) to convert cell-specific NFRs to *nifH*-specific rates. To avoid underestimating the contributions of *Trichodesmium* and Hets to NFRs, which exhibit high variability in cellular *nifH* copy numbers, moderate polyploidy factors were applied. For UCYN-C and γ-24774A11, a polyploidy factor of 1 was assumed due to limited data. Cell-specific NFRs for most phylotypes were calculated as means from published datasets (Shao et al., 2023). Cell-specific NFR for UCYN-C was derived from the average ¹⁵N₂ assimilation rates reported for its host *Epithemia pelagica*, normalized to a 15-hour daily fixation period (Schvarcz et al., 2022). For γ-24774A11, the cell-specific NFR was estimated based on the average NFR of the symbiosis with its diatom host, assuming one host diatom per four γ-24774A11 cells (Tschitschko et al., 2024). — no data.

L375: The spring value of 58.5 seems incorrect; re-check Table S3.

Response:

We thank the Reviewer for the comment. After re-calculating the NFR estimates, we have revised the spring value in Table S6 (formerly Table S3) and updated the manuscript accordingly.

Line 508-509: “Given the depth-integrated diazotroph abundances, the averaged NFRs in the ECS ranged from 29.51 μmol N m⁻² d⁻¹ in spring to 44.14 μmol N m⁻² d⁻¹ in autumn (Table S6).”.

L376: Because this study directly measured surface N₂-fixation rates as well, author should verify consistency with values inferred from *nifH* copies and per-cell rates and measured rates by incubations; otherwise the subsequent quantitative discussion can be not-reliable.

Response:

We thank the Reviewer for the comment. We have added a comparison between the estimated and

measured NFRs in Figure S8 and included the relevant discussion in the revised manuscript.

Line 504-508: “Under these assumptions, the estimated and measured surface NFRs were highly correlated (Slope = 1.04, $R^2 = 0.39$, $p < 0.001$; Fig. S8). Despite the uncertainties and low level of explained variance (Fig. S8), the significantly positive correlation between the two approaches support the validity of using cell-specific NFRs in assessing regional N budget.”.

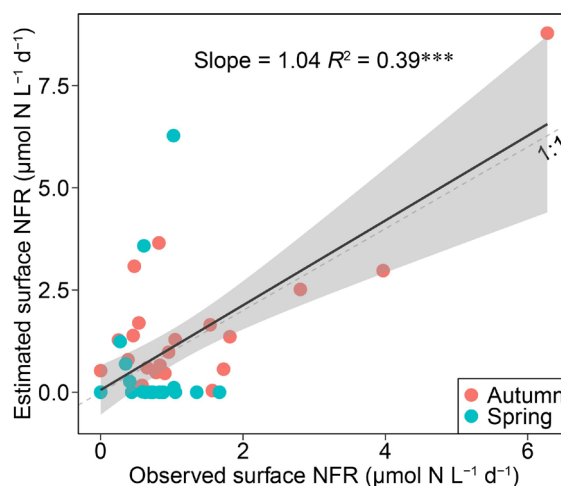


Figure S8. Linear regression of estimated versus measured surface N_2 fixation rates (NFRs). Estimates were derived from cell-specific NFRs, *nifH* gene polyploidy, and phylotype-specific *nifH* gene abundance. The shaded area represents the 95% confidence interval.

L399: Is this broad niche of *Trichodesmium* consistent with the earlier claim of an r-strategy for *Trichodesmium*?

Response:

We thank the Reviewer for the comment. We realized that the use of the term “r-strategy” might be inappropriate and could potentially lead to conceptual ambiguity. Therefore, we have removed all the descriptions that characterize *Trichodesmium* as an r-strategist in the revised manuscript.

L399–404: Of course there is intra- and inter-specific metabolic variability; explain how such variability could produce the observed differences.

Response:

We thank the Reviewer for the comment. We have added the discussion on how intra- and inter-specific metabolic variability in *Trichodesmium* could account for the expanded NO_x niche breadth in the revised manuscript.

Line 541-547: “Specifically, intra-specific plasticity may enable endemic *Trichodesmium* populations to modulate N₂ fixation and growth by exploiting ambient SRP under fluctuating NO_x regimes (Knapp et al., 2012; Knapp, 2012), or utilizing NO_x directly (Boatman et al., 2018). Meanwhile, inter-specific distributions of *Trichodesmium* were evident, with *T. erythraeum* dominating coastal waters whereas *T. thiebautii* prevailing on the ECS shelf (Jiang et al., 2018; Zhang et al., 2019), possibly owing to species-specific physiological optima and NO_x tolerance thresholds (Carpenter et al., 1993; Confesor et al., 2022; Rodier and Le Borgne, 2008, 2010).”.

L411–412: Zehr et al. (2007) did not study genotype-specific optimal temperatures. Webb et al. (2009) reported an optimum of 26–30 °C, which is not as broad and is inconsistently higher than current result (<24 °C).

Response:

We thank the Reviewer for the comment. We have revised the sentence and incorporated additional evidence from the literature.

Line 563-569: “The latter seems in contrast to the well-known preference of UCYN-B for warm, oligotrophic waters (Jiang et al., 2025; Webb et al., 2009). Nevertheless, global metadata analysis suggests that UCYN-B may survive under low temperatures (20–23°C) and high NO_x (up to 20 µM) and SRP levels (1–2 µM) (Tang and Cassar, 2019). Both field and laboratory studies have shown that UCYN-B remains viable under nitrate-rich conditions (5–20 µM) when SRP is sufficient (Knapp et al., 2012; Knapp, 2012; Turk-Kubo et al., 2018). These results indicate that UCYN-B has the capacity to cope with lower temperatures and elevated nutrient concentrations.”.

L414: Brum et al. 2015 analyzed diatom-associated diazotrophs, please discuss it?

Response:

We thank the Reviewer for the comment. We have added the discussion comparing our results on diatom-associated diazotrophs with those reported in Brum et al. (2015) in the revised manuscript.

Line 579-590: “Compared with the niche conditions suitable for open-ocean populations (temperature: 24.2°C; NO_x: 1.38 µM) (Brun et al., 2015), Hets inhabited niches of slightly higher temperature but lower NO_x levels (Fig. 8A and C). This result is different from previous findings based on studies analyzing all the *Richelia* diatom hosts, including *Rhizosolenia clevei* (Het-1 host),

Hemiaulus hauckii (Het-2 host) and *H. membranaceus* (Brun et al., 2015; Luo et al., 2012), which may have distinct temperature and nutrient optima (Stenegren et al., 2017; Tuo et al., 2014, 2021). In fact, the different niche preferences for temperature and SRP between Het-1 and Het-2 were verified in this study (Fig. 8A and D), as well as in other studies (Foster et al., 2007; Tuo et al., 2021; Stenegren et al., 2017). Furthermore, the modeled realized niche space based on regional environmental gradients (e.g., temperature: 17.6–27.6°C) may be narrower than that derived from global datasets (16.5–31.6°C) (Brun et al., 2015; Jiang et al., 2025; Tang and Cassar, 2019). Thus, the prediction of realized niche of Hets may be affected by a variety of factors, including physiological traits of the diazotrophs, their hosts, and the scale of spatial sampling.”.

K420-425: Please refer Tschitschko et al. 2024 which report important ecology and physiology of γ -24774A11.

Response:

We thank the Reviewer for the comment. We have incorporated additional information on the ecology and physiology of γ -24774A11 and its diatom host in the revised manuscript.

Line 590-599: “Finally, our niche modeling result suggests a cosmopolitan distribution of γ -24774A11 in oligotrophic surface waters (Fig. 8) (Cheung et al., 2020; Shiozaki et al., 2018; Tschitschko et al., 2024), despite the fact that it is frequently found in environments with elevated NO_x concentrations (Bird and Wyman, 2013; Shao and Luo, 2022; Shiozaki et al., 2014). This feature may be related to its diatom host, which acquires a substantial fraction of fixed nitrogen from γ -24774A11 (Tschitschko et al., 2024). Nevertheless, in high-NO_x environments, the host might leverage ambient NO_x for growth, thereby partially reducing its metabolic dependency on the symbiont. To illuminate the mechanisms governing the biogeographic distribution of the γ -24774A11-diatom association (Cornejo-Castillo and Zehr, 2021; Shao and Luo, 2022; Tschitschko et al., 2024), more systematic studies are needed.”.

L432: To my knowledge, Cheung et al. 2019 did not mention ecological niche similarity between UCYN-C and Hets.

Response:

We thank the Reviewer for the comment. We have removed the citation of Cheung et al. (2019) in

the sentence.

L438–439: Cabello et al. (2016) did not report a distinct “reproductive strategy” for UCYN-A.

Response:

We thank the Reviewer for the comment. We have removed the statement accordingly.

L440: Cabello et al. (2016) speculated on such a strategy, but many opposing studies also exist: UCYN-A2 is considered coastal ecotype, whereas UCYN-A1 is open-ocean ecotype (e.g., Turk-Kubo et al. 2017, 2021; Henke et al. 2018). Cite a more objective literature rather than only studies consistent with your results.

Response:

We thank the Reviewer for the comment. We have revised the manuscript to include a more balanced perspective by including references to studies (Henke et al., 2018; Turk-Kubo et al., 2017, 2021) that describe distinct distribution patterns of UCYN-A.

Line 551-560: “It has been suggested that UCYN-A1 is an open-ocean ecotype and UCYN-A2 a coastal ecotype (Henke et al., 2018; Turk-Kubo et al., 2017, 2021). However, we found a co-occurrence pattern between these two ecotypes, with UCYN-A2/A3/A4 exhibiting lower abundance and narrower vertical distribution range (Fig. 3 and S4M–P) (Cabello et al., 2016; G  rikas Ribeiro et al., 2018; Wen et al., 2022). The distinct UCYN-A2 distributions between this and previous studies may be due to the phenotypical plasticity of the UCYN-A2-haptophyte symbioses, allowing them to inhabit either in the oligotrophic open oceans with small cell appearance (4–5 µm) or large one (7–10 µm) in the eutrophic coastal regions (Cabello et al., 2016; Hagino et al., 2013). Although genes related to N₂ fixation and energy production are actively transcribed in both UCYN-A ecotypes, the mechanisms underlying their niche overlap and differentiation require further studies (Mu  oz-Mar  n et al., 2023; Nguyen et al., 2025).”.

Figures

Figure 4: Clarify whether data represent an average across multiple stations and include error bars if so.

Response:

We thank the Reviewer for the comment. We have updated the Figure 4 caption to clarify that the

data represent “average abundances” and have added error lines to the figure.

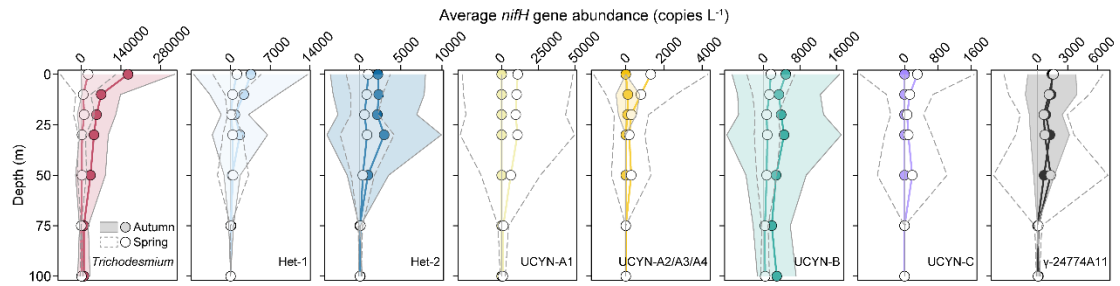


Figure 4. Vertical distributions in the average abundances of the eight major diazotrophic phylotypes in the East China Sea during autumn and spring as determined based on the TaqMan qPCR assay of the *nifH* gene. The grey solid and dashed lines represent ± 1 standard deviation for autumn and spring, respectively.

Figures 5 and 6: The numbers near the pie/bar charts appear to be station numbers—please clarify in the captions.

Response:

We thank the Reviewer for the comment. We have added the description of station numbers to the captions of Figures 5 and 6.

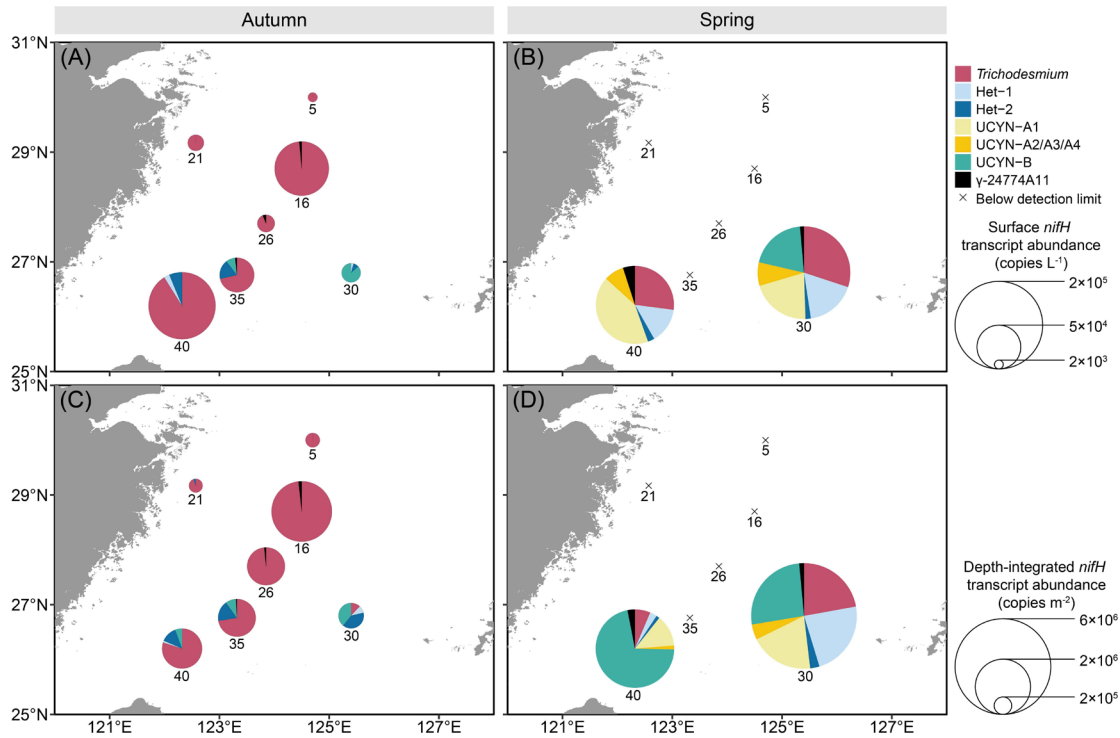


Figure 5. Surface (A, B) and depth-integrated (C, D) abundances of the seven major diazotrophic phylotypes in the East China Sea during autumn and spring as determined based on TaqMan qPCR assay of the *nifH* transcript (i.e., RNA-based). Note that the transcript abundance of UCYN-B was derived from nighttime samples, whereas that of

the other groups was from daytime samples. The depth-integrated transcript abundance was calculated based on the integration of the upper 50 m of the water columns. The station numbers are positioned adjacent to corresponding pie charts and crossover points. Land topography was obtained from the General Bathymetric Chart of the Oceans (GEBCO, <https://www.gebco.net/>, last access: 24 January 2025).

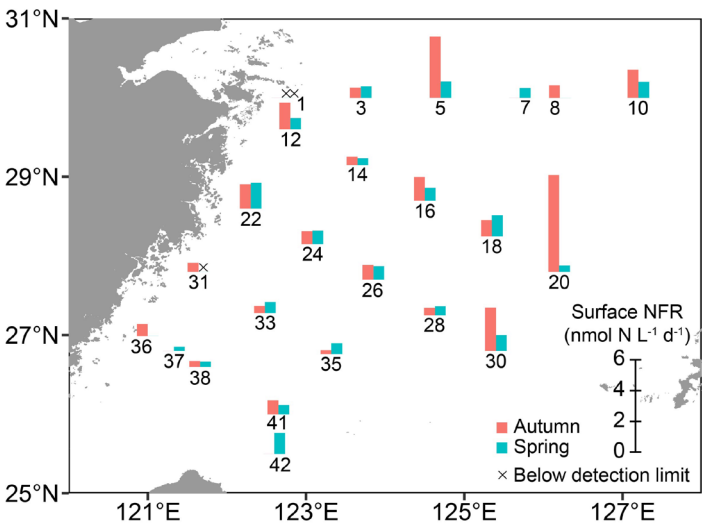


Figure 6. N₂ fixation rates in surface waters at designated stations in the East China Sea during autumn and spring as determined with in situ isotope tracing. The station numbers are positioned adjacent to corresponding bar charts and crossover points. Sampling excluded stations 7, 37 and 42 in autumn, and stations 8 and 36 in spring. Land topography was obtained from the General Bathymetric Chart of the Oceans (GEBCO, <https://www.gebco.net/>, last access: 24 January 2025).

Figure 3: If station numbers are important here, add them for consistency.

Response:

We thank the Reviewer for the comment. We have added the station numbers to Figure 3 and clarified them in the caption.

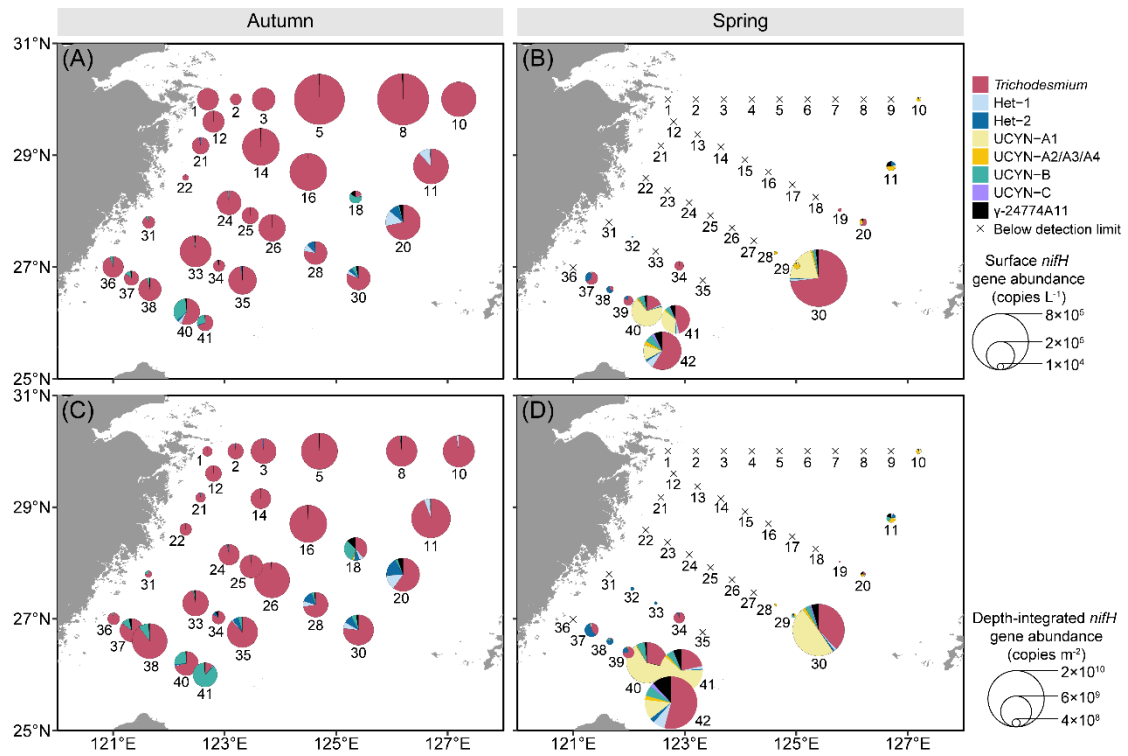


Figure 3. Surface (A, B) and depth-integrated (C, D) abundances of the eight major diazotrophic phylotypes in the East China Sea during autumn and spring as determined based on the quantification of the *nifH* gene (i.e., DNA-based) with TaqMan qPCR. The station numbers are positioned adjacent to corresponding pie charts and crossover points. Land topography was obtained from the General Bathymetric Chart of the Oceans (GEBCO, <https://www.gebco.net/>, last access: 24 January 2025).

References

- Berman-Frank, I., Cullen, J. T., Shaked, Y., Sherrell, R. M., and Falkowski, P. G.: Iron availability, cellular iron quotas, and nitrogen fixation in *Trichodesmium*, *Limnol. Oceanogr.*, 46, 1249–1260, <https://doi.org/10.4319/lo.2001.46.6.1249>, 2001.
- Bird, C., and Wyman, M.: Transcriptionally active heterotrophic diazotrophs are widespread in the upper water column of the Arabian Sea, *FEMS Microbiol. Ecol.*, 84, 189–200, <https://doi.org/10.1111/1574-6941.12049>, 2013.
- Boatman, T. G., Davey, P. A., Lawson, T., and Geider, R. J.: The physiological cost of diazotrophy for *Trichodesmium erythraeum* IMS101, *PLoS One*, 13, e0195638, <https://doi.org/10.1371/journal.pone.0195638>, 2018.
- Brun, P., Vogt, M., Payne, M. R., Gruber, N., O'Brien, C. J., Buitenhuis, E. T., Le Quéré, C., Leblanc, K., and Luo, Y.: Ecological niches of open ocean phytoplankton taxa, *Limnol. Oceanogr.*, 60, 1020–1038, <https://doi.org/10.1002/lno.10074>, 2015.
- Cabello, A. M., Cornejo-Castillo, F. M., Raho, N., Blasco, D., Vidal, M., Audic, S., De Vargas, C., Latasa, M., Acinas, S. G., and Massana, R.: Global distribution and vertical patterns of a prymnesiophyte–cyanobacteria obligate symbiosis, *ISME J.*, 10, 693 – 706, <https://doi.org/10.1038/ismej.2015.147>, 2016.
- Carpenter, E., O'Neil, J., Dawson, R., Siddiqui, P., Roenneberg, T., and Bergman, B.: The tropical diazotrophic phytoplankter *Trichodesmium*: biological characteristics of two common species, *Mar. Ecol. Prog. Ser.*, 95, 295–304, <https://doi.org/10.3354/meps095295>, 1993.
- Carpenter, E. J., Subramaniam, A., and Capone, D. G.: Biomass and primary productivity of the cyanobacterium *Trichodesmium* spp. in the tropical N Atlantic ocean, *Deep-Sea Res. Pt. I*, 51, 173–203, <https://doi.org/10.1016/j.dsr.2003.10.006>, 2004.
- Chen, M., Lu, Y., Jiao, N., Tian, J., Kao, S., and Zhang, Y.: Biogeographic drivers of diazotrophs in the western Pacific Ocean, *Limnol. Oceanogr.*, 64, 1403–1421, <https://doi.org/10.1002/lno.11123>, 2019.
- Cheung, S., Suzuki, K., Saito, H., Umezawa, Y., Xia, X., and Liu, H.: Highly heterogeneous diazotroph communities in the Kuroshio current and the Tokara Strait, Japan, *PLoS One*, 12, e0186875, <https://doi.org/10.1371/journal.pone.0186875>, 2017.
- Cheung, S., Suzuki, K., Xia, X., and Liu, H.: Transportation of diazotroph community from the upstream to downstream of the Kuroshio, *J. Geophys. Res.-Biogeo.*, 124, 2680–2693,

- <https://doi.org/10.1029/2018JG004960>, 2019.
- Cheung, S., Nitanai, R., Tsurumoto, C., Endo, H., Nakaoka, S., Cheah, W., Lorda, J. F., Xia, X., Liu, H., and Suzuki, K.: Physical forcing controls the basin-scale occurrence of nitrogen-fixing organisms in the North Pacific Ocean, *Glob. Biogeochem. Cycles*, 34, e2019GB006452, <https://doi.org/10.1029/2019GB006452>, 2020.
- Church, M. J., Short, C. M., Jenkins, B. D., Karl, D. M., and Zehr, J. P.: Temporal patterns of nitrogenase gene (*nifH*) expression in the oligotrophic North Pacific Ocean, *Appl. Environ. Microbiol.*, 71, 5362–5370, <https://doi.org/10.1128/AEM.71.9.5362-5370.2005>, 2005b.
- Coale, T. H., Loconte, V., Turk-Kubo, K. A., Vanslebrouck, B., Mak, W. K. E., Cheung, S., Ekman, A., Chen, J.-H., Hagino, K., Takano, Y., Nishimura, T., Adachi, M., Le Gros, M., Larabell, C., and Zehr, J. P.: Nitrogen-fixing organelle in a marine alga, *Science*, 384, 217–222, <https://doi.org/10.1126/science.adk1075>, 2024.
- Confesor, K. A., Selden, C. R., Powell, K. E., Donahue, L. A., Mellett, T., Caprara, S., Knapp, A. N., Buck, K. N., and Chappell, P. D.: Defining the realized niche of the two major clades of *Trichodesmium*: A study on the West Florida Shelf, *Front. Mar. Sci.*, 9, 821655, <https://doi.org/10.3389/fmars.2022.821655>, 2022.
- Cornejo-Castillo, F. M. and Zehr, J. P.: Intriguing size distribution of the uncultured and globally widespread marine non-cyanobacterial diazotroph Gamma-A, *ISME J.*, 15, 124–128, <https://doi.org/10.1038/s41396-020-00765-1>, 2021.
- Cornejo-Castillo, F. M., Inomura, K., Zehr, J. P., and Follows, M. J.: Metabolic trade-offs constrain the cell size ratio in a nitrogen-fixing symbiosis, *Cell*, S009286742400182X, <https://doi.org/10.1016/j.cell.2024.02.016>, 2024.
- Deng, L., Cheung, S., Kang, C., Liu, K., Xia, X., and Liu, H.: Elevated temperature relieves phosphorus limitation of marine unicellular diazotrophic cyanobacteria, *Limnol. Oceanogr.*, 67, 122–134, <https://doi.org/10.1002/lno.11980>, 2022.
- Foster, R. A., Subramaniam, A., Mahaffey, C., Carpenter, E. J., Capone, D. G., and Zehr, J. P.: Influence of the Amazon River plume on distributions of free-living and symbiotic cyanobacteria in the western tropical north Atlantic Ocean, *Limnol. Oceanogr.*, 52, 517–532, <https://doi.org/10.4319/lo.2007.52.2.0517>, 2007.
- Fu, F., Yu, E., Garcia, N., Gale, J., Luo, Y., Webb, E. A., and Hutchins, D. A.: Differing responses of

- marine N₂ fixers to warming and consequences for future diazotroph community structure, *Aquat. Microb. Ecol.*, 72, 33–46, <https://doi.org/10.3354/ame01683>, 2014.
- Garcia, N. S., Fu, F.-X., Breene, C. L., Yu, E. K., Bernhardt, P. W., Mulholland, M. R., and Hutchins, D. A.: Combined effects of CO₂ and light on large and small isolates of the unicellular N₂-fixing cyanobacterium *Crocospaera watsonii* from the western tropical Atlantic Ocean, *Eur. J. Phycol.*, 48, 128–139, <https://doi.org/10.1080/09670262.2013.773383>, 2013.
- Gérikas Ribeiro, C., Lopes Dos Santos, A., Marie, D., Pereira Brandini, F., and Vaultot, D.: Small eukaryotic phytoplankton communities in tropical waters off Brazil are dominated by symbioses between Haptophyta and nitrogen-fixing cyanobacteria, *ISME J.*, 12, 1360–1374, <https://doi.org/10.1038/s41396-018-0050-z>, 2018.
- Goebel, N. L., Turk, K. A., Achilles, K. M., Paerl, R., Hewson, I., Morrison, A. E., Montoya, J. P., Edwards, C. A., and Zehr, J. P.: Abundance and distribution of major groups of diazotrophic cyanobacteria and their potential contribution to N₂ fixation in the tropical Atlantic Ocean: Diazotrophic cyanobacteria in the tropical North Atlantic, *Environ. Microbiol.*, 12, 3272–3289, <https://doi.org/10.1111/j.1462-2920.2010.02303.x>, 2010.
- Gradoville, M. R., Bombar, D., Crump, B. C., Letelier, R. M., Zehr, J. P., and White, A. E.: Diversity and activity of nitrogen-fixing communities across ocean basins, *Limnol. Oceanogr.*, 62, 1895–1909, <https://doi.org/10.1002/lno.10542>, 2017.
- Gradoville, M. R., Cabello, A. M., Wilson, S. T., Turk-Kubo, K. A., Karl, D. M., and Zehr, J. P.: Light and depth dependency of nitrogen fixation by the non-photosynthetic, symbiotic cyanobacterium UCYN-A, *Environ. Microbiol.*, 23, 4518–4531, <https://doi.org/10.1111/1462-2920.15645>, 2021.
- Guo, L., Chen, Y., Wang, F., Meng, X., Xu, Z., and Zhuang, G.: Effects of Asian dust on the atmospheric input of trace elements to the East China Sea, *Mar. Chem.*, 163, 19–27, <https://doi.org/10.1016/j.marchem.2014.04.003>, 2014.
- Hagino, K., Onuma, R., Kawachi, M., and Horiguchi, T.: Discovery of an endosymbiotic nitrogen-fixing cyanobacterium UCYN-A in *Braarudosphaera bigelowii* (Prymnesiophyceae), *PLoS One*, 8, e81749, <https://doi.org/10.1371/journal.pone.0081749>, 2013.
- Henke, B. A., Turk-Kubo, K. A., Bonnet, S., and Zehr, J. P.: Distributions and abundances of sublineages of the N₂-fixing cyanobacterium *Candidatus Atelocyanobacterium thalassa* (UCYN-A) in the New Caledonian Coral Lagoon, *Front. Microbiol.*, 9, 554, <https://doi.org/10.3389/fmicb.2018.00554>,

2018.

- Irwin, A. J., Nelles, A. M., and Finkel, Z. V.: Phytoplankton niches estimated from field data, *Limnol. Oceanogr.*, 57, 787–797, <https://doi.org/10.4319/lo.2012.57.3.0787>, 2012.
- Jiang, R., Hong, H., Wen, Z., Yu, X., Browning, T. J., Chen, Z., Shang, Y., Liu, X., Cao, Z., Achterberg, E. P., Dai, M., and Shi, D.: Significant contribution of the unicellular cyanobacterium UCYN-B to oceanic nitrogen fixation, *Natl. Sci. Rev.*, 12, nwaf337, <https://doi.org/10.1093/nsr/nwaf337>, 2025.
- Jiang, Z., Chen, J., Zhou, F., Zhai, H., Zhang, D., and Yan, X.: Summer distribution patterns of *Trichodesmium* spp. in the Changjiang (Yangtze River) Estuary and adjacent East China Sea shelf, *Oceanologia*, 59, 248–261, <https://doi.org/10.1016/j.oceano.2017.02.001>, 2017.
- Jiang, Z., Li, H., Zhai, H., Zhou, F., Chen, Q., Chen, J., Zhang, D., and Yan, X.: Seasonal and spatial changes in *Trichodesmium* associated with physicochemical properties in East China Sea and southern Yellow Sea, *J. Geophys. Res.-Biogeo.*, 123, 509–530, <https://doi.org/10.1002/2017JG004275>, 2018.
- Jiang, Z., Chen, J., Zhai, H., Zhou, F., Yan, X., Zhu, Y., Xuan, J., Shou, L., and Chen, Q.: Kuroshio shape composition and distribution of filamentous diazotrophs in the East China Sea and southern Yellow Sea, *J. Geophys. Res.-Oceans*, 124, 7421–7436, <https://doi.org/10.1029/2019JC015413>, 2019.
- Jiang, Z., Zhu, Y., Sun, Z., Zhai, H., Zhou, F., Yan, X., Zeng, J., Chen, J., and Chen, Q.: Enhancement of summer nitrogen fixation by the Kuroshio intrusion in the East China Sea and southern Yellow Sea, *J. Geophys. Res.-Biogeo.*, <https://doi.org/10.1029/2022JG007287>, 2023a.
- Jiang, Z., Zhu, Y., Sun, Z., Zhai, H., Zhou, F., Yan, X., Chen, Q., Chen, J., and Zeng, J.: Size-fractionated N₂ fixation off the Changjiang Estuary during summer, *Front. Microbiol.*, 14, 1189410, <https://doi.org/10.3389/fmicb.2023.1189410>, 2023b.
- Kantor, E. J. H., Robicheau, B. M., Tolman, J., Archibald, J. M., and LaRoche, J.: Metagenomics reveals the genetic diversity between sublineages of UCYN-A and their algal host plastids, *ISME Commun.*, 4, ycae150, <https://doi.org/10.1093/ismeco/ycae150>, 2024.
- Knapp, A., Dekaezemacker, J., Bonnet, S., Sohm, J., and Capone, D.: Sensitivity of *Trichodesmium erythraeum* and *Crocospaera watsonii* abundance and N₂ fixation rates to varying NO₃[−] and PO₄^{3−} concentrations in batch cultures, *Aquat. Microb. Ecol.*, 66, 223–236, <https://doi.org/10.3354/ame01577>, 2012.

- Knapp, A. N.: The sensitivity of marine N₂ fixation to dissolved inorganic nitrogen, *Front. Microbiol.*, 3, 374, <https://doi.org/10.3389/fmicb.2012.00374>, 2012.
- Lee Chen, Y., Chen, H., and Lin, Y.: Distribution and downward flux of *Trichodesmium* in the South China Sea as influenced by the transport from the Kuroshio current, *Mar. Ecol. Prog. Ser.*, 259, 47–57, <https://doi.org/10.3354/meps259047>, 2003.
- Lee Chen, Y., Chen, H.-Y., Lin, Y.-H., Yong, T.-C., Taniuchi, Y., and Tuo, S.: The relative contributions of unicellular and filamentous diazotrophs to N₂ fixation in the South China Sea and the upstream Kuroshio, *Deep-Sea Res. Pt. I*, 85, 56–71, <https://doi.org/10.1016/j.dsr.2013.11.006>, 2014.
- Lu, Y., Wen, Z., Shi, D., Lin, W., Bonnet, S., Dai, M., and Kao, S.: Biogeography of N₂ fixation influenced by the western boundary current intrusion in the South China Sea, *J. Geophys. Res.-Oceans*, 124, 6983–6996, <https://doi.org/10.1029/2018jc014781>, 2019.
- Luo, Y.-W., Doney, S. C., Anderson, L. A., Benavides, M., Berman-Frank, I., Bode, A., Bonnet, S., Boström, K. H., Böttjer, D., Capone, D. G., Carpenter, E. J., Chen, Y. L., Church, M. J., Dore, J. E., Falcón, L. I., Fernández, A., Foster, R. A., Furuya, K., Gómez, F., Gundersen, K., Hynes, A. M., Karl, D. M., Kitajima, S., Langlois, R. J., LaRoche, J., Letelier, R. M., Marañón, E., McGillicuddy, D. J., Moisander, P. H., Moore, C. M., Mouriño-Carballido, B., Mulholland, M. R., Needoba, J. A., Orcutt, K. M., Poulton, A. J., Rahav, E., Raimbault, P., Rees, A. P., Riemann, L., Shiozaki, T., Subramaniam, A., Tyrrell, T., Turk-Kubo, K. A., Varela, M., Villareal, T. A., Webb, E. A., White, A. E., Wu, J., and Zehr, J. P.: Database of diazotrophs in global ocean: abundance, biomass and nitrogen fixation rates, *Earth Syst. Sci. Data*, 4, 47–73, <https://doi.org/10.5194/essd-4-47-2012>, 2012.
- Moisander, P. H., Serros, T., Paerl, R. W., Beinart, R. A., and Zehr, J. P.: Gammaproteobacterial diazotrophs and *nifH* gene expression in surface waters of the South Pacific Ocean, *ISME J.*, 8, 1962–1973, <https://doi.org/10.1038/ismej.2014.49>, 2014.
- Montoya, J. P., Voss, M., Hler, P. K., and Capone, D. G.: A simple, high-precision, high-sensitivity tracer assay for N₂ fixation, *Appl. Environ. Microbiol.*, 62, 986–993, <https://doi.org/10.1128/aem.62.3.986-993.1996>, 1996.
- Muñoz-Marín, M. D. C., Magasin, J. D., and Zehr, J. P.: Open ocean and coastal strains of the N₂-fixing cyanobacterium UCYN-A have distinct transcriptomes, *PLoS One*, 18, e0272674, <https://doi.org/10.1371/journal.pone.0272674>, 2023.

- Nguyen, A., Ustick, L. J., Larkin, A. A., and Martiny, A. C.: Global phylogeography and microdiversity of the marine diazotrophic cyanobacteria *Trichodesmium* and UCYN-A, *mSphere*, 10, e00245-25, <https://doi.org/10.1128/msphere.00245-25>, 2025.
- Phillips, S. J., Anderson, R. P., and Schapire, R. E.: Maximum entropy modeling of species geographic distributions, *Ecol. Model.*, 190, 231–259, <https://doi.org/10.1016/j.ecolmodel.2005.03.026>, 2006.
- Rodier, M., and Le Borgne, R.: Population dynamics and environmental conditions affecting *Trichodesmium* spp. (filamentous cyanobacteria) blooms in the south–west lagoon of New Caledonia, *J. Exp. Mar. Biol. Ecol.*, 358, 20–32, <https://doi.org/10.1016/j.jembe.2008.01.016>, 2008.
- Rodier, M., and Le Borgne, R.: Population and trophic dynamics of *Trichodesmium thiebautii* in the SE lagoon of New Caledonia. Comparison with *T. erythraeum* in the SW lagoon, *Mar. Pollut. Bull.*, 61, 349–359, <https://doi.org/10.1016/j.marpolbul.2010.06.018>, 2010.
- Sato, T., Yamaguchi, T., Hidataka, K., Sogawa, S., Setou, T., Kodama, T., Shiozaki, T., and Takahashi, K.: Grazing mortality as a controlling factor in the uncultured non-cyanobacterial diazotroph (Gamma A) around the Kuroshio region, *Biogeosciences*, 22, 625–639, <https://doi.org/10.5194/bg-22-625-2025>, 2025.
- Schvarcz, C. R., Wilson, S. T., Caffin, M., Stancheva, R., Li, Q., Turk-Kubo, K. A., White, A. E., Karl, D. M., Zehr, J. P., and Steward, G. F.: Overlooked and widespread pennate diatom-diazotroph symbioses in the sea, *Nat. Commun.*, 13, 799, <https://doi.org/10.1038/s41467-022-28065-6>, 2022.
- Schvarcz, C. R., Stancheva, R., Turk-Kubo, K. A., Wilson, S. T., Zehr, J. P., Edwards, K. F., Steward, G. F., Archibald, J. M., Oatley, G., Sinclair, E., Santos, C., Paulini, M., Aunin, E., Gettle, N., Niu, H., McKenna, V., O'Brien, R., Wellcome Sanger Institute Tree of Life Management, Samples and Laboratory Team, Wellcome Sanger Institute Scientific Operations: Sequencing Operations, Wellcome Sanger Institute Tree of Life Core Informatics Team, EBI Aquatic Symbiosis Genomics Data Portal Team, and Aquatic Symbiosis Genomics Project Leadership: The genome sequences of the marine diatom *Epithemia pelagica* strain UHM3201 (Schvarcz, Stancheva & Steward, 2022) and its nitrogen-fixing, endosymbiotic cyanobacterium, *Wellcome Open Res.*, 9, 232, <https://doi.org/10.12688/wellcomeopenres.21534.1>, 2024.
- Shao, Z., and Luo, Y.-W.: Controlling factors on the global distribution of a representative marine non-cyanobacterial diazotroph phylotype (Gamma A), *Biogeosciences*, 19, 2939–2952, <https://doi.org/10.5194/bg-19-2939-2022>, 2022.

Shao, Z., Xu, Y., Wang, H., Luo, W., Wang, L., Huang, Y., Agawin, N. S. R., Ahmed, A., Benavides, M., Bentzon-Tilia, M., Berman-Frank, I., Berthelot, H., Biegala, I. C., Bif, M. B., Bode, A., Bonnet, S., Bronk, D. A., Brown, M. V., Campbell, L., Capone, D. G., Carpenter, E. J., Cassar, N., Chang, B. X., Chappell, D., Chen, Y. L., Church, M. J., Cornejo-Castillo, F. M., Detoni, A. M. S., Doney, S. C., Dupouy, C., Estrada, M., Fernandez, C., Fernández-Castro, B., Fonseca-Batista, D., Foster, R. A., Furuya, K., Garcia, N., Goto, K., Gago, J., Gradoville, M. R., Hamersley, M. R., Henke, B. A., Hörstmann, C., Jayakumar, A., Jiang, Z., Kao, S.-J., Karl, D. M., Kittu, L. R., Knapp, A. N., Kumar, S., LaRoche, J., Liu, H., Liu, J., Lory, C., Löscher, C. R., Marañón, E., Messer, L. F., Mills, M. M., Mohr, W., Moisander, P. H., Mahaffey, C., Moore, R., Mouriño-Carballido, B., Mulholland, M. R., Nakaoka, S., Needoba, J. A., Raes, E. J., Rahav, E., Ramírez-Cárdenas, T., Reeder, C. F., Riemann, L., Riou, V., Robidart, J. C., Sarma, V. V. S. S., Sato, T., Saxena, H., Selden, C., Seymour, J. R., Shi, D., Shiozaki, T., Singh, A., Sipler, R. E., Sun, J., Suzuki, K., Takahashi, K., Tan, Y., Tang, W., Tremblay, J.-É., Turk-Kubo, K., Wen, Z., White, A. E., Wilson, S. T., Yoshida, T., Zehr, J. P., Zhang, R., Zhang, Y., and Luo, Y.-W.: Global oceanic diazotroph database version 2 and elevated estimate of global oceanic N₂ fixation, *Earth Syst. Sci. Data*, 15, 3673–3709, <https://doi.org/10.5194/essd-15-3673-2023>, 2023.

Shen, H., Wan, X. S., Zou, W., Dai, M., Xu, M. N., and Kao, S.-J.: Light-driven integration of diazotroph-derived nitrogen in euphotic nitrogen cycle, *Nat. Commun.*, 15, 9193, <https://doi.org/10.1038/s41467-024-53067-x>, 2024.

Shiozaki, T., Ijichi, M., Kodama, T., Takeda, S., and Furuya, K.: Heterotrophic bacteria as major nitrogen fixers in the euphotic zone of the Indian Ocean, *Glob. Biogeochem. Cycles*, 28, 1096–1110, <https://doi.org/10.1002/2014GB004886>, 2014.

Shiozaki, T., Takeda, S., Itoh, S., Kodama, T., Liu, X., Hashihama, F., and Furuya, K.: Why is *Trichodesmium* abundant in the Kuroshio? *Biogeosciences*, 12, 6931–6943, <https://doi.org/10.5194/bg-12-6931-2015>, 2015.

Shiozaki, T., Kondo, Y., Yuasa, D., and Takeda, S.: Distribution of major diazotrophs in the surface water of the Kuroshio from northeastern Taiwan to south of mainland Japan, *J. Plankton Res.*, 40, 407–419, <https://doi.org/10.1093/plankt/fby027>, 2018.

Stenegren, M., Berg, C., Padilla, C. C., David, S.-S., Montoya, J. P., Yager, P. L., and Foster, R. A.: Piecewise structural equation model (SEM) disentangles the environmental conditions favoring

- diatom diazotroph associations (DDAs) in the Western Tropical North Atlantic (WTNA), *Front. Microbiol.*, 8, 810, <https://doi.org/10.3389/fmicb.2017.00810>, 2017.
- Stenegren, M., Caputo, A., Berg, C., Bonnet, S., and Foster, R. A.: Distribution and drivers of symbiotic and free-living diazotrophic cyanobacteria in the western tropical South Pacific, *Biogeosciences*, 15, 1559–1578, <https://doi.org/10.5194/bg-15-1559-2018>, 2018.
- Su, H., Yang, R., Zhang, A., and Li, Y.: Dissolved iron distribution and organic complexation in the coastal waters of the East China Sea, *Mar. Chem.*, 173, 208–221, <https://doi.org/10.1016/j.marchem.2015.03.007>, 2015.
- Tang, W., and Cassar, N.: Data-driven modeling of the distribution of diazotrophs in the global ocean, *Geophys. Res. Lett.*, 46, 12258–12269, <https://doi.org/10.1029/2019GL084376>, 2019.
- Tschitschko, B., Esti, M., Philippi, M., Kidane, A. T., Littmann, S., Kitzinger, K., Speth, D. R., Li, S., Kraberg, A., Tienken, D., Marchant, H. K., Kartal, B., Milucka, J., Mohr, W., and Kuypers, M. M. M.: Rhizobia–diatom symbiosis fixes missing nitrogen in the ocean, *Nature*, 630, 899–904, <https://doi.org/10.1038/s41586-024-07495-w>, 2024.
- Tuo, S., Chen, Y., and Chen, H.: Low nitrate availability promotes diatom diazotroph associations in the marginal seas of the western Pacific, *Aquat. Microb. Ecol.*, 73, 135–150, <https://doi.org/10.3354/ame01715>, 2014.
- Tuo, S.-H., Mulholland, M. R., Chen, Y.-L. L., Chappell, P. D., and Chen, H.-Y.: Patterns in *Rhizosolenia*- and *Guinardia*-associated *Richelia* abundances in the tropical marginal seas of the western North Pacific, *J. Plankton Res.*, 43, 338–352, <https://doi.org/10.1093/plankt/fbab022>, 2021.
- Turk-Kubo, K. A., Achilles, K. M., Serros, T. R. C., Ochiai, M., Montoya, J. P., and Zehr, J. P.: Nitrogenase (*nifH*) gene expression in diazotrophic cyanobacteria in the tropical North Atlantic in response to nutrient amendments, *Front. Microbiol.*, 3, <https://doi.org/10.3389/fmicb.2012.00386>, 2012.
- Turk-Kubo, K. A., Farnelid, H. M., Shilova, I. N., Henke, B., and Zehr, J. P.: Distinct ecological niches of marine symbiotic N₂-fixing cyanobacterium *Candidatus Atelocyanobacterium thalassa* sublineages, *J. Phycol.*, 53, 451–461, <https://doi.org/10.1111/jpy.12505>, 2017.
- Turk-Kubo, K. A., Connell, P., Caron, D., Hogan, M. E., Farnelid, H. M., and Zehr, J. P.: In situ diazotroph population dynamics under different resource ratios in the North Pacific Subtropical Gyre, *Front. Microbiol.*, 3, 386, <https://doi.org/10.3389/fmicb.2018.01616>, 2018.

- Turk-Kubo, K. A., Mills, M. M., Arrigo, K. R., van Dijken, G., Henke, B. A., Stewart, B., Wilson, S. T., and Zehr, J. P.: UCYN-A/haptophyte symbioses dominate N₂ fixation in the Southern California Current System, *ISME Commun.*, 1, 42, <https://doi.org/10.1038/s43705-021-00039-7>, 2021.
- Vélez-Belchí, P., Centurioni, L. R., Lee, D.-K., Jan, S., and Niiler, P. P.: Eddy induced Kuroshio intrusions onto the continental shelf of the East China Sea, *J. Mar. Res.*, 71, 83–107, <https://doi.org/10.1357/002224013807343470>, 2013.
- Webb, E. A., Ehrenreich, I. M., Brown, S. L., Valois, F. W., and Waterbury, J. B.: Phenotypic and genotypic characterization of multiple strains of the diazotrophic cyanobacterium, *Crocospaera watsonii*, isolated from the open ocean, *Environ. Microbiol.*, 11, 338–348, <https://doi.org/10.1111/j.1462-2920.2008.01771.x>, 2009.
- Wen, Z., Browning, T. J., Cai, Y., Dai, R., Zhang, R., Du, C., Jiang, R., Lin, W., Liu, X., Cao, Z., Hong, H., Dai, M., and Shi, D.: Nutrient regulation of biological nitrogen fixation across the tropical western North Pacific, *Sci. Adv.*, 8, eabl7564, <https://doi.org/10.1126/sciadv.abl7564>, 2022.
- Wu, C., Fu, F.-X., Sun, J., Thangaraj, S., and Pujari, L.: Nitrogen fixation by *Trichodesmium* and unicellular diazotrophs in the northern South China Sea and the Kuroshio in summer, *Sci. Rep.*, 8, 2415, <https://doi.org/10.1038/s41598-018-20743-0>, 2018.
- Xiao, W., Wang, L., Laws, E., Xie, Y., Chen, J., Liu, X., Chen, B., and Huang, B.: Realized niches explain spatial gradients in seasonal abundance of phytoplankton groups in the South China Sea, *Prog. Oceanogr.*, 162, 223–239, <https://doi.org/10.1016/j.pocean.2018.03.008>, 2018.
- Yang, H., Cai, J., Wu, L., Guo, H., Chen, Z., Jing, Z., and Gan, B.: The intensifying East China Sea Kuroshio and disappearing Ryukyu Current in a warming climate, *Geophys. Res. Lett.*, 51, e2023GL106944, <https://doi.org/10.1029/2023GL106944>, 2024.
- Yin, M., Li, X., Xiao, Z., and Li, C.: Relationships between intensity of the Kuroshio current in the East China Sea and the East Asian winter monsoon, *Acta Oceanol. Sin.*, 37, 8–19, <https://doi.org/10.1007/s13131-018-1240-2>, 2018.
- Yue, J., Noman, M. A., and Sun, J.: Kuroshio intrusion drives the *Trichodesmium* assemblage and shapes the phytoplankton community during spring in the East China Sea, *J. Oceanol. Limnol.*, 39, 536–549, <https://doi.org/10.1007/s00343-020-9344-x>, 2021.
- Zhang, H., Qin, Y., Deng, B., Cheng, X., and Jiang, X.: Distribution characteristics of *Trichodesmium* in the East China Sea, *J. Appl. Oceanogr.*, 38, 246–251, <https://doi.org/10.3969/J.ISSN.2095->

4972.2019.02.012, 2019.

Zhong, Y., Liu, X., Xiao, W., Laws, E. A., Chen, J., Wang, L., Liu, S., Zhang, F., and Huang, B.:
Phytoplankton community patterns in the Taiwan Strait match the characteristics of their realized
niches, *Prog. Oceanogr.*, 186, 102366, <https://doi.org/10.1016/j.pocean.2020.102366>, 2020.